AD NUMBER
AD905666
LIMITATION CHANGES
TO: **Approved for public release; distribution is unlimited.**
FROM: **Distribution authorized to U.S. Gov't. agencies only; Test and Evaluation; DEC 1972. Other requests shall be referred to Air Force Flight Dynamics Laboratory, Attn: FER, Wright-Patterson AFB, OH 45433.**
AUTHORITY
AFWAl ltr, 24 Jun 1980

AEDC-TR-72-171

cy. 2

DRAG, PERFORMANCE CHARACTERISTICS, AND PRESSURE DISTRIBUTIONS OF SEVERAL RIGID AERODYNAMIC DECELERATORS AT MACH NUMBERS FROM 0.2 TO 5

R. W. Rhudy and S. S. Baker

ARO, Inc.

December 1972

VON KÁRMÁN GAS DYNAMICS FACILITY
ARNOLD ENGINEERING DEVELOPMENT CENTER
AIR FORCE SYSTEMS COMMAND
ARNOLD AIR FORCE STATION, TENNESSEE

NOTICES

When U. S. Government drawings specifications, or other data are used for any purpose other than a definitely related Government procurement operation, the Government thereby incurs no responsibility nor any obligation whatsoever, and the fact that the Government may have formulated, furnished, or in any way supplied the said drawings, specifications, or other data, is not to be regarded by implication or otherwise, or in any manner licensing the holder or any other person or corporation, or conveying any rights or permission to manufacture, use, or sell any patented invention that may in any way be related thereto.

Qualified users may obtain copies of this report from the Defense Documentation Center.

References to named commercial products in this report are not to be considered in any sense as an endorsement of the product by the United States Air Force or the Government.

DRAG, PERFORMANCE CHARACTERISTICS, AND PRESSURE DISTRIBUTIONS OF SEVERAL RIGID AERODYNAMIC DECELERATORS AT MACH NUMBERS FROM 0.2 TO 5

R. W. Rhudy and S. S. Baker
ARO, Inc.

FOREWORD

The work reported herein was conducted by the Arnold Engineering Development Center (AEDC) under sponsorship of the Air Force Flight Dynamics Laboratory (AFFDL), Recovery and Crew Station Branch (FER), under Program Element 62201F.

The results presented were obtained by ARO, Inc. (a subsidiary of Sverdrup & Parcel and Associates, Inc.), contract operator of AEDC, Air Force Systems Command (AFSC), Arnold Air Force Station, Tennessee. The tests were conducted from April 25 through May 5, 1972, under ARO Project No. VA011. The final data reduction was completed on June 15, 1972, and the manuscript was submitted for publication on July 28, 1972.

This technical report has been reviewed and is approved.

JIMMY W. MULLINS
Lt Colonel, USAF
Chief Air Force Test Director, VKF
Directorate of Test

A. L. COAPMAN
Colonel, USAF
Director of Test

ABSTRACT

Static force and pressure distribution tests were conducted at Mach numbers from 0.2 to 5.0 on rigid models of several aerodynamic decelerators in the wake of three types of forebodies. The tests were conducted at decelerator pitch angles from -8 to 8 deg at nominal free-stream dynamic pressures of 0.5, 1.0, 1.5, and 2.0 psia. The decelerators were positioned at various axial stations in the wake of the forebodies, and selected configurations were tested in the free stream (no forebody). Data are presented showing the effects of Mach numbers, decelerator pitch angle, and location in the wake on the drag and stability of various decelerator configurations. The pressure data support the measured force data and show large fluctuations in the canopy internal pressure on the supersonic X-2 parachute design.

CONTENTS

APPENDIXES

I. ILLUSTRATIONS

Figure

NOMENCLATURE

A	Reference area, 50.27 in.^{2} for 8-in. supersonic X-2 model, 19.63 in.^{2} for 5-in. supersonic X-2 model, 24.63 in.^{2} for Hemisflo model, and 22.90 in.^{2} for 45-deg cone model
C_A	Total axial-force coefficient, total axial force/$q_\infty A$
C_{A_o}	Total axial-force coefficient at zero pitch angle
C_m	Pitching-moment coefficient, pitching moment/$q_\infty A d_1$
C_{m_α}	Initial slope of pitching-moment curve, $(dC_m/d\alpha)_{\alpha = 0}$

C_N	Normal-force coefficient, normal force/$q_\infty A$
C_{N_α}	Initial slope of normal-force curve, $(dC_N/d\alpha)_{\alpha = 0}$
C_p	Pressure coefficient, $(p - p_\infty)/q_\infty$
d	Forebody reference dimension used to nondimensionalize the decelerator-forebody longitudinal separation distance (see Fig. 3), in.
d_1	Decelerator reference length, 5.0 in. for 5-in. supersonic X-2 model, 8.0 in. for 8-in. supersonic X-2 model, 5.6 in. (nominal design diameter) for Hemisflo model, and 5.4 in. for 45-deg cone model
f	Frequency of pressure variations, Hz
ℓ	Distance from lip of X-2 decelerator to trailing edge (see Fig. 2), in.
M.R.	Moment reference location
M_∞	Free-stream Mach number
p	Surface pressure, psia
p_o	Tunnel stilling chamber pressure, psia
p_∞	Free-stream static pressure, psia
Δp	Amplitude of pressure variations at $x_p/\ell = 0.735$
q_∞	Free-stream dynamic pressure, psia
Re/in.	Free-stream Reynolds number per inch
T_o	Tunnel stilling chamber temperature, °R
x	Distance from forebody reference point to leading edge of decelerator (see Fig. 3), in.
x'	Distance from center of rotation to leading edge of decelerator, measured along decelerator axis (see Fig. 3), in.
x_p	Distance from lip of X-2 decelerator to pressure orifice, measured along decelerator axis (see Fig. 2), in.
z_p	Perpendicular distance from decelerator axis to pressure orifice (see Fig. 2), in.
α	Decelerator pitch angle, deg
ϕ	Roll angle of pressure orifice rays on supersonic X-2 decelerator pressure models (see Fig. 2), deg

SECTION I
INTRODUCTION

An experimental investigation was conducted in the 40-in. Supersonic Wind Tunnel (A) of the von Kármán Gas Dynamics Facility (VKF) to determine the drag and static-stability coefficients and surface pressures of a number of rigid aerodynamic decelerators. The decelerators were tested at several positions in the wake of three forebodies which were supported by a strut spanning the tunnel test section. The tests were conducted at free-stream Mach numbers from 0.2 to 5 at free-stream dynamic pressures from 0.5 to 2.0 psia (simulated pressure altitudes up to 130,000 ft). These tests are a follow-on to a previous investigation of rigid aerodynamic decelerators conducted in Tunnel A (Ref. 1).

Results are presented to show the effects of Mach number, dynamic pressure, decelerator pitch angle, and location in the wake on the drag and stability of various decelerator configurations. Corresponding results for the surface pressure distributions are also presented. A complete test summary is given in the tables.

SECTION II
APPARATUS

2.1 TEST ARTICLES

2.1.1 Forebody Models and Support

The forebody support consisted of a full-tunnel-span strut with wedge-shaped (total angle of 18 deg) leading and trailing edges and a total thickness of 0.312 in. A small span of cylindrical leading edge, just upstream of the forebody, was exposed when the ejection seat was installed.

The forebodies were a 2.00-in.-diam cone-cylinder with a 13-deg half-angle sharp cone nose, a simulated ejection seat and man, and a simulated crew-ejection module (Fig. 1, Appendix I). Selected configurations were tested in the free stream with the forebody-strut combination removed from the tunnel.

2.1.2 Decelerator Models

The tests were conducted on four basic decelerator models: two rigid models (an 8-in.-diam and a 5-in.-diam) of a parachute design designated "Supersonic X-2," a 45-deg sharp cone, and a rigid model of a hemispherical parachute design designated "Hemisflo."

The 45-deg sharp cone and the 5-in.-diam X-2 force models were designed and fabricated by VKF and were used only for the static force tests. The cone had a base diameter of 5.40 in.

The two rigid X-2 pressure models were obtained from contours specified by AFFDL. The 8-in.-diam pressure model was modified after the pressure phase and used to obtain force data. The simulated parachute canopy of the 5-in. model had a leading-edge outside diameter (OD) of 4.00 in., an exit (trailing-edge) OD of 1.50 in., and maximum OD of 5.00 in. A full set of contours is given in table form in Fig. 2a. Six removable internal webs and twelve suspension lines were provided for each model. The 5-in. model was tested alone, with the lines, and with the lines and webs. The 8-in. model had dimensions 1.6 times as large as the 5-in. model except as shown in Fig. 2b. The 8-in. model was tested alone and with lines. Both X-2 decelerator models, when used for pressure data, were instrumented with nine external and eight internal surface static pressure taps and one internal tap to measure pressure oscillations. The orifice locations are shown in Fig. 2a. The balance attachment for both models was located below the centerline of the canopy to minimize the flow disturbance from the attachment and to allow flow through the canopy exit.

The Hemisflo decelerator was also obtained from contours specified by AFFDL. The hemispherical parachute canopy had a leading-edge of 3.342 in. and a maximum OD of 3.500 in. The canopy contained 16 sets of machined slots with dimensions as shown in Fig. 2c. Sixteen suspension lines were permanently attached to the canopy. A full set of contours is given in table form in Fig. 2c. The balance attachment was located at the back of the canopy on the axis of symmetry.

All the decelerator configurations were tested on the same six-component balance, which was attached by means of an offset strut to a mechanism that provided remote positioning in the vertical and longitudinal direction. This mechanism was attached to the standard Tunnel A model mounting equipment which provides remote positioning of the model in pitch.

A schematic showing the relationship of the decelerators to the forebodies is shown in Fig. 3, and photographs of the models and test installation are given in Fig. 4.

2.2 INSTRUMENTATION

Tunnel A stilling chamber pressure is measured with 150- and 300-psid transducers referenced to a near vacuum and having full-scale calibrated ranges of 10, 50, 150, and 300 psi. Based on periodic comparisons with secondary standards, the precision of these transducers (a band which includes 95 percent of the residuals) is estimated to be ±0.5 percent of the reading but no better than 0.015 psid. Stilling chamber temperature is measured with a copper-constantan thermocouple to a precision of ±0.5 percent or ±0.75°F, whichever is larger, based on thermocouple wire manufacturer's specifications.

The model surface pressures were measured with 15-psid transducers that are referenced to a near vacuum and have full-scale calibrated ranges of 1, 5, and 15 psi. Based on periodic comparisons with secondary standards, the precision of these transducers is estimated to be ±0.3 percent of full scale for the 1-psid range, and ±0.2 percent of full scale for the 5- and 15-psid ranges. The pressure oscillations at $x_p/\ell = 0.735$ were measured with a 1-psia, fast-response, strain-gage transducer developed by the VKF which has a frequency response up to 1000 Hz to a precision of ±0.02 psi and ±1.0 percent of the measured frequency.

Model forces and moments were measured with a six-component, moment-type, strain-gage balance supplied and calibrated by VKF. Before testing, static loads in each plane and combined static loads were applied to the balance, simulating the range of model loads anticipated for the test. The following uncertainties represent the bands for 95 percent of the measurement residuals based on differences between applied loads and the corresponding values calculated from the final data reduction equations:

Balance Components	Design Load	Range of Static Loads	Measurement Uncertainty
Normal Force, lb	200	±60	±0.3
Pitching Moment, in.-lb	680	±90	±0.5
Axial Force, lb	100	0 to 100	±0.2

The transfer distance to the decelerator model moment reference point (4.478 in. for the 5-in. Supersonic X-2, 7.015 in. for the 8-in. Supersonic X-2, 3.827 in. for the Hemisflo decelerator, and 1.604 in. for the 45-deg sharp cone) was measured with a precision of ±0.010 in.

2.3 WIND TUNNEL

Tunnel A is a continuous, closed-circuit, variable-density wind tunnel with an automatically driven flexible-plate-type nozzle and a 40- by 40-in. test section. The tunnel can be operated at Mach numbers from 1.5 to 6 at maximum stagnation pressures from 29 to 200 psia, respectively, and stagnation temperatures up to 750°R (M_∞ = 6). Minimum operating pressures range from about one-tenth to one-twentieth of the maximum at each Mach number. The model may be injected into the tunnel for a test run and then retracted for model changes without interrupting the tunnel flow. A description of the tunnel and airflow calibration information may be found in Ref. 2.

Tunnel A has also been calibrated at subsonic Mach numbers from 0.2 to 0.8. Mach numbers within the range from 0.2 to 0.8 are set by monitoring tunnel sidewall static pressures in conjunction with the diffuser geometry.

SECTION III
TEST PROCEDURE

3.1 TEST CONDITIONS AND METHODS

The tests were conducted at nominal free-stream Mach numbers from 0.2 to 5.0 at nominal free-stream dynamic pressures (q_∞) of 0.5, 1.0, 1.5, and 2.0 psia. The test conditions are given in Table I (Appendix II), and a complete test summary for both the force and pressure phases of the investigation is given in Table II.

Before injection into the tunnel the models were adjusted for zero roll to within ±0.1 deg using an inclinometer. After the decelerator models were injected into the airflow, zero pitch was set within ±0.05 deg using an optical level and reference points on the models. All other pitch angles were set to within ±0.1 deg using the standard tunnel pitch mechanism. The decelerators were positioned on the horizontal center-

line of the forebody wake by use of the remote positioning mechanism and an optical level and in the desired x/d position by a combination of this mechanism and the tunnel injection mechanism. A fixed distance (x') between the center of rotation and the decelerator (see Fig. 3) was maintained at angle of attack. The estimated precision of the model position was ±0.005 in. in the vertical direction (z) and ±0.050 in. in the longitudinal direction (x).

Decelerator yaw alignment was checked prior to each operating shift and found to be within ±0.5 deg for all configurations. During these checks the spanwise alignment of the decelerators to the forebodies was also adjusted to within ±0.015 in. over the entire range of x/d.

The data were obtained in the following sequence for any given combination of configuration, Mach number, and dynamic pressure: The decelerator was positioned at zero angle of attack and maximum x/d. Data were then obtained as x/d was decreased to the minimum and, in selected cases, returned to the maximum. For the force phase, a ptich polar was then obtained at selected x/$\bar{d}$'s as x/d was decreased.

3.2 UNCERTAINTIES OF THE DATA

Uncertainties in the basic tunnel parameters (p_O and M_∞) were estimated from repeat calibrations of the instrumentation and from repeatability and uniformity of the test section flow during tunnel calibrations. These uncertainties were then used to estimate the uncertainties in other free-stream properties, using the Taylor series method to define the error propagation.

Nominal M_∞	Nominal q_∞	Uncertainty (Percent ±)			
		M_∞	p_O	p_∞	q_∞
0.2 to 0.8	0.5 to 1.0	1.9 to 0.2	0.5	0.1 to 0.3	1.7 to 0.5
1.5	1.0	0.7	↓	1.5	0.5
2.0	1.0	0.5	↓	1.6	0.8
2.5	1.0	0.3	↓	1.3	0.8
3.0	1.0	0.4	↓	1.9	1.1
3.5	1.0	0.3	↓	1.5	1.0
4.0	0.5 to 2.0	0.5	↓	2.7	1.7
5.0	1.0	0.3	↓	1.9	1.3

The maximum uncertainties listed below are for the aerodynamic coefficients obtained on the Supersonic X-2 decelerator models for q_∞ = 1.0 psia. A more detailed list of uncertainties may be found in Ref. 1. These values are considered to be typical for all configurations.

X.XXX = Maximum Absolute Uncertainty (±) near Minimum Load
(X.X) = Maximum Percentage Uncertainty (±) at Maximum Load

C_N	C_m	C_A
0.003	0.004	0.008
(1.5)	(4.2)	(1.2)

The uncertainties listed below are for the pressure coefficients obtained on the various condigurations of the 5-in., X-2 decelerator model and the 8-in., X-2 decelerator model with lines.

Nominal Test Conditions		Uncertainty (Percent ±)	
M_∞	q_∞	At Maximum C_p	At Minimum C_p
2.0	1.0	1.24	2.24
3.0	1.0	1.40	3.19
4.0	0.5	1.92	9.66
4.0	1.0	1.95	5.74
4.0	1.5	2.01	3.62
5.0	1.0	1.42	5.42

SECTION IV
RESULTS AND DISCUSSION

At the request of AFFDL, and in keeping with the previous decelerator test, the data were obtained at constant dynamic pressure levels and are so presented. Corresponding unit Reynolds numbers for each M_∞ and q_∞ condition are listed in Table I. In the discussion which follows, only general comments on the test results are made, and these are primarily restricted to the various summary figures which are pre-

sented for each test phase. A detailed analysis of these results will be made by AFFDL/FER.

4.1 DECELERATOR FORCE DATA

Unless otherwise noted, the Supersonic X-2 chute models are without webs. The effects of Mach number and angle of attack on the normal-force, pitching-moment, and axial-force characteristics of the various decelerator configurations are shown in Figs. 5 to 9. It should be noted that the reference diameter for the Hemisflo decelerator was the nominal design diameter of 5.6 in., not the actual diameter of 3.5 in. In general, the effect of increasing Mach number for a given configuration at a given x/d was to decrease the axial-force and normal-force coefficients at all pitch angles. However, the pitching moment was essentially insensitive to changes in Mach number. While the X-2 configurations displayed positive static longitudinal stability in the wake of all forebodies (Figs. 5 through 7), the pitching-moment coefficients for the Hemisflo (Fig. 8) and 45-deg conical (Fig. 9) decelerators were near zero for all test conditions.

The data for the crew module forebody show that the 45-deg cone produced the largest axial-force coefficient and the Hemisflo produced the smallest. The results for the two sizes of X-2 behind the crew module (Figs. 5c and 7) show sizable differences in C_N and C_A over most of the pitch range. One obvious reason for the differences must be the large difference in the size of the decelerators (capture area) compared with the size of the wake of the forebody. As noted for the 5-in. X-2 in Ref. 1, the 8-in. X-2 with the lines removed produced higher values of axial force than with the lines installed (Figs. 5a and 6).

The data for all configurations in the wake of either the ejection seat or the crew module forebodies show that the normal force was not zero angle of attack, which is a result of the nonsymmetrical wake produced by these forebodies. Again, because of the larger capture area relative to the wake, the 8-in. X-2 was the least affected. This nonsymmetry of the wake is clearly shown in the schlieren photographs (Fig. 10).

The slopes of the normal-force and pitching-moment coefficients (stability derivatives) as a function of Mach number, along with the axial-force coefficient at zero angle of attack for the various decele-

rators, are shown in Fig. 11. These data show more clearly the reduction in axial force with an increase in Mach number in the supersonic range and the relative magnitudes for the various configurations. As expected, because of the smaller model with a larger porosity, the Hemisflo decelerator gave axial-force and normal-force coefficients well below the X-2 for the same conditions. The axial-force coefficient in the free stream was always higher for this decelerator than when in the wake of the forebody. In the subsonic range, the axial-force coefficient changed very little with Mach number increase and was nearly the same for all decelerators in the wake of the crew module. The subsonic level was well below the supersonic level for the X-2; however, it was very nearly the maximum on the Hemisflo decelerator. Some of the data contained in this figure are from Ref. 1.

The trends of the stability derivatives near zero pitch angle as a function of Mach number are quite mixed. The mixed results in the wake of the ejection seat and the crew module were not unexpected, however, in light of unsymmetrical wakes and the large differences in size of the decelerators.

4.2 DECELERATOR PRESSURE DATA

Zero pitch angle pressure distributions on several configurations of the supersonic X-2 decelerator in the wake of the cone-cylinder forebody are presented in Fig. 12. Only small variations on the forward portion of the canopy were obtained in the external pressure distributions regardless of configuration, x/d, or Mach number. The internal pressure distributions indicate a general increase in overall level whenever x/d was increased or Mach number was decreased. These data, if pressure integrations were performed, would give the same trends in axial force with Mach number that were shown in the force data of Fig. 11a, particularly the large decrease obtained in C_{A_o} for the 8-in. model between $M_\infty = 3$ and 5.

Pressure data are presented in Fig. 13 for the 5-in. X-2 in the free stream. These data when viewed as proportional to axial force indicate little variation in C_A with Mach number increase on the decelerator without lines, and for the decelerator with lines, indicate that the axial force would decrease as Mach number is increased from 2.0 to 4.0 and then remain essentially constant at $M_\infty = 4.0$ and 5.0. These trends are in agreement with the force data of Ref. 1, the results of which, for the decelerator with lines, were included in Fig. 11c.

Data obtained from the dynamic pressure transducer located at an x_p/ℓ of 0.735 are presented in Fig. 14. These data show that, in general, the decelerator in the free stream with the lines removed had relatively low amplitude and low frequency pressure fluctuations. The amplitude of the pressure fluctuation was increased, except at $M_\infty = 2$, by as much as 200 percent, and the frequency increased by about a factor of four to approximately 600 Hz when this configuration was tested in the wake of the cone-cylinder. When the lines were added to the decelerator in the wake of the cone-cylinder, the amplitude of the pressure fluctuations increased dramatically, while the frequency decreased only slightly except at $M_\infty = 5$, where both frequency and amplitude dropped to values less than obtained on this configuration in the free stream. The results for $x/d = 9.0$ at this Mach number (solid symbol), however, show a frequency level as high as obtained at the lower Mach numbers for $x/d = 7.0$ although the amplitude was still small relative to the peak obtained at $M_\infty = 4.0$.

SECTION V
CONCLUDING REMARKS

The data within this report are presented to give some insight into the performance that could be expected from several types and configurations of decelerators in the wake of three typical forebodies. This report is not meant to give a thorough analysis of the various problems involved; however, some of the more important conclusions that can be derived from these data, in addition to those from the preceding test, are as follows:

1. Data obtained on two sizes of Supersonic X-2 decelerator were in disagreement, probably a result of the differences in capture area.
2. Supersonically, the Hemisflo decelerator gave values of axial-force coefficient generally lower than the X-2.
3. The subsonic axial-force coefficient was higher than was the supersonic for the Hemisflo decelerator, whereas the reverse was true for the X-2.
4. The pressure distribution data indicated the same trends in axial force, as did the force data from previous tests.

5. Large amplitude internal pressure fluctuations were present whenever the full configuration X-2 was tested in the wake of the cone-cylinder, except at $M_\infty = 5$.

REFERENCES

1. Rhudy, R. W. and Jones, J. H. "Drag and Performance Characteristics of Several Rigid Aerodynamic Decelerators at Mach Numbers from 1.5 to 6." AEDC-TR-71-233 (AD889022), November 1971.

2. Test Facilities Handbook (Ninth Edition). "von Karman Gas Dynamics Facility, Vol. 3." Arnold Engineering Development Center, July 1971.

APPENDIXES

I. ILLUSTRATIONS

II. TABLES

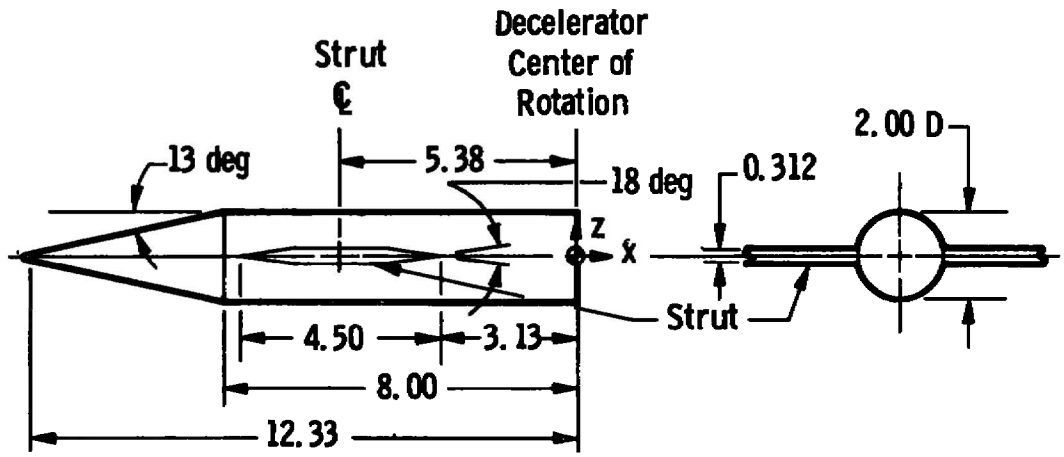

a. Cone-Cylinder Forebody

All Dimensions in Inches (Not to Scale)

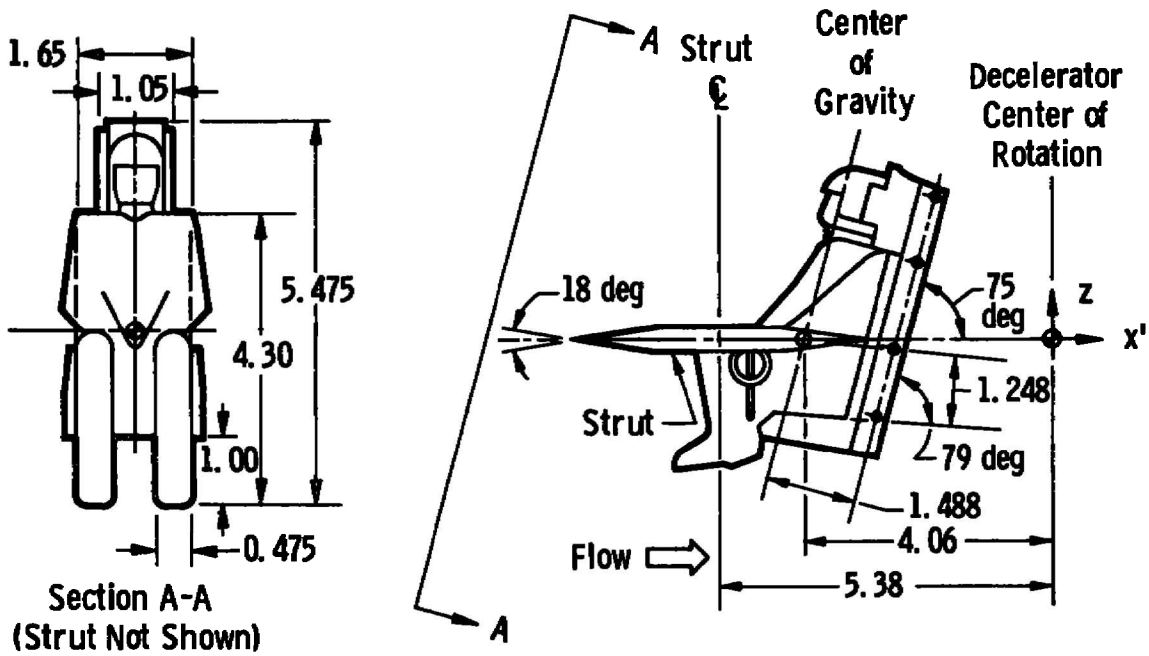

b. Ejection-Seat Forebody

Fig. 1 Forebody Details

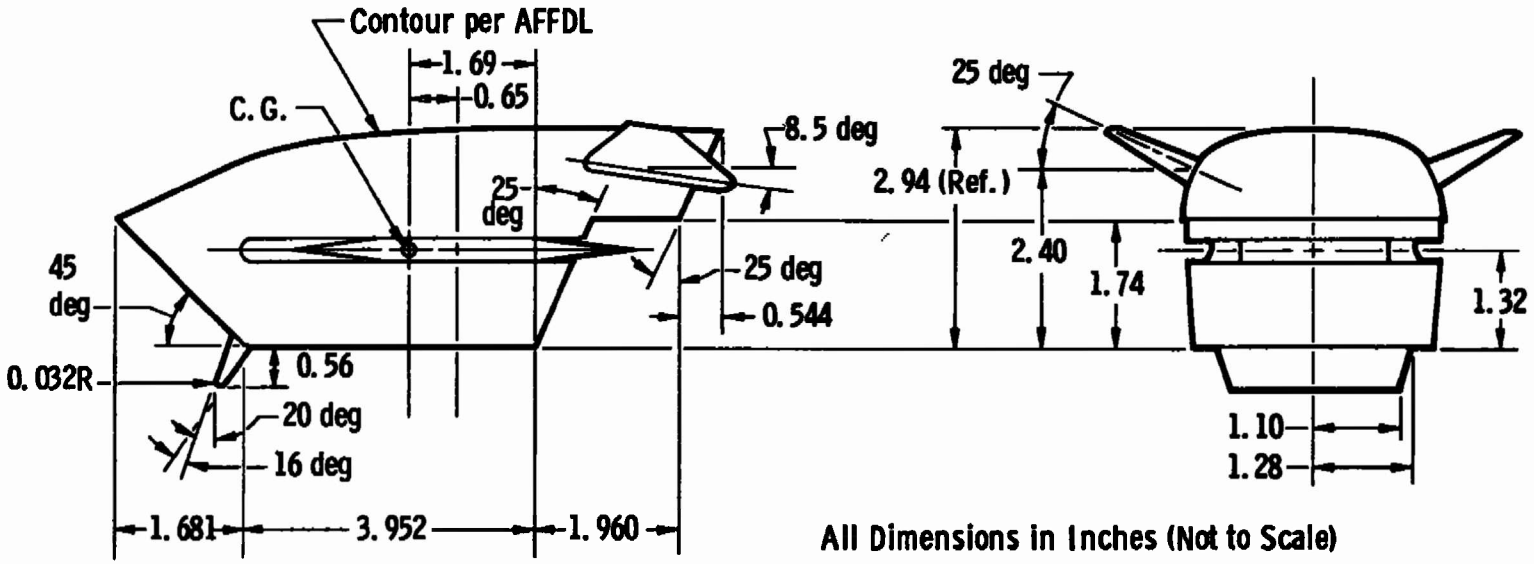

c. Crew Module Forebody

Fig. 1 Concluded

Canopy Profile Coordinates					
X_p, in.	Z_p, in.	X_p, in.	Z_p, in.	X_p, in.	Z_p, in.
0	2.000	1.50	2.483	2.75	1.938
0.25	2.105	1.68	2.500	3.00	1.535
0.50	2.205	1.75	2.495	3.25	1.070
0.75	2.290	2.00	2.435	3.50	0.840
1.00	2.370	2.25	2.338	3.75	0.763
1.25	2.438	2.50	2.183	3.88	0.750

Orifice Locations					
ϕ, deg	X_p	X_p/ℓ	ϕ	X_p	X_p/ℓ
75	0.25	0.064	*255	0.50	0.129
75	0.50	0.129	*255	1.00	0.258
75	1.00	0.258	*255	1.50	0.387
75	1.50	0.387	*255	2.00	0.516
75	2.00	0.516	*255	2.00	0.516
*75	2.00	0.516	*255	2.50	0.645
75	2.50	0.645	*255	3.00	0.774
75	3.00	0.774	*255	3.50	0.903
75	3.50	0.903			
*Denotes Internal Tap					

Dynamic Pressure Tap at X_p/ℓ = 0.735 (Internal)

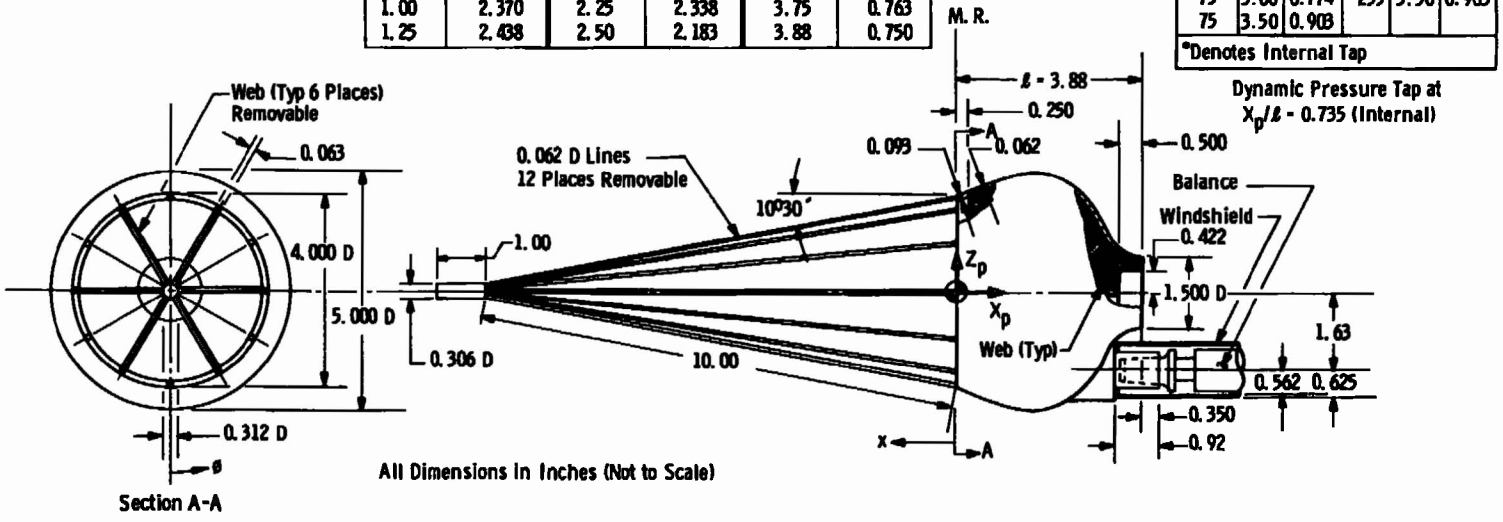

a. Five-Inch Supersonic X-2 Decelerator

Fig. 2 Decelerator Details

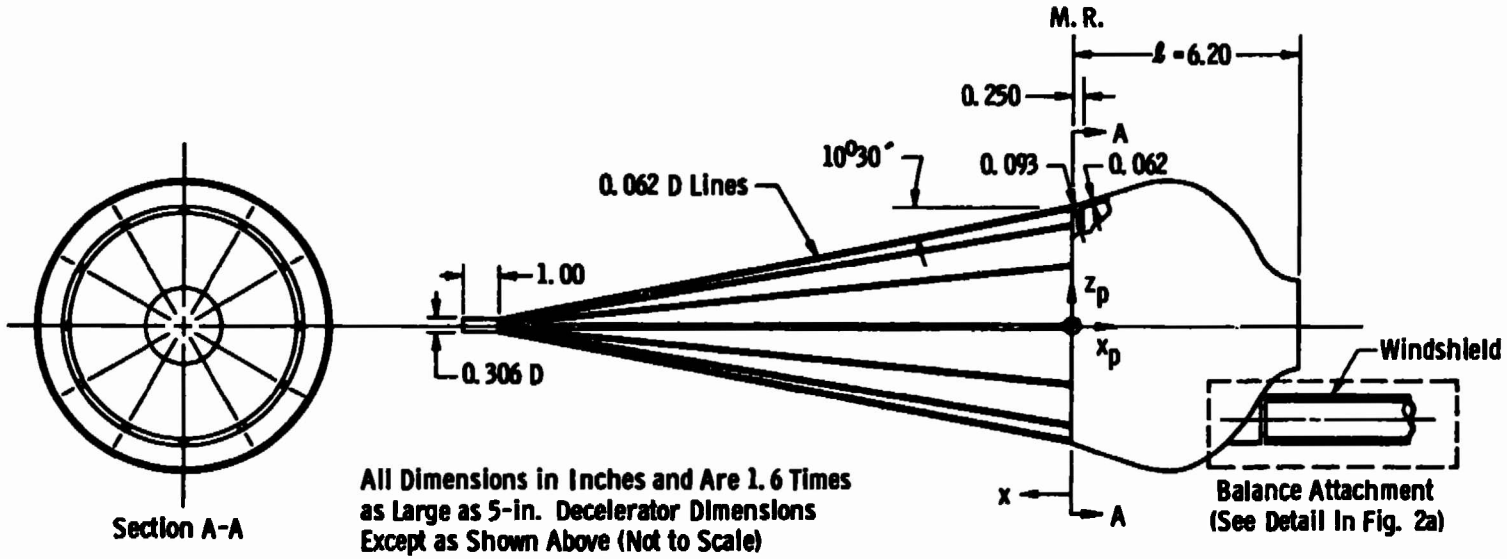

b. Eight-Inch Supersonic X-2 Decelerator
Fig. 2 Continued

Slot No.	1	2	3	4	5	6	7	8	9	10
'L'	0.475	0.485	0.500	0.483	0.480	0.425	0.365	0.280	0.205	0.120

Note: Design Geometric Porosity = 16.9 percent

Canopy Profile Coordinates			
x_p	z_p	x_p	z_p
0.000	1.671	1.313	1.643
0.088	1.698	1.400	1.608
0.175	1.715	1.488	1.566
0.263	1.729	1.575	1.514
0.350	1.734	1.663	1.461
0.438	1.741	1.750	1.400
0.525	1.747	1.838	1.316
0.613	1.748	1.925	1.216
0.700	1.750	2.013	1.094
0.788	1.747	2.100	0.957
0.875	1.741	2.188	0.772
0.963	1.731	2.231	0.656
1.050	1.719	2.275	0.490
1.138	1.701	2.319	0.000
1.225	1.677		

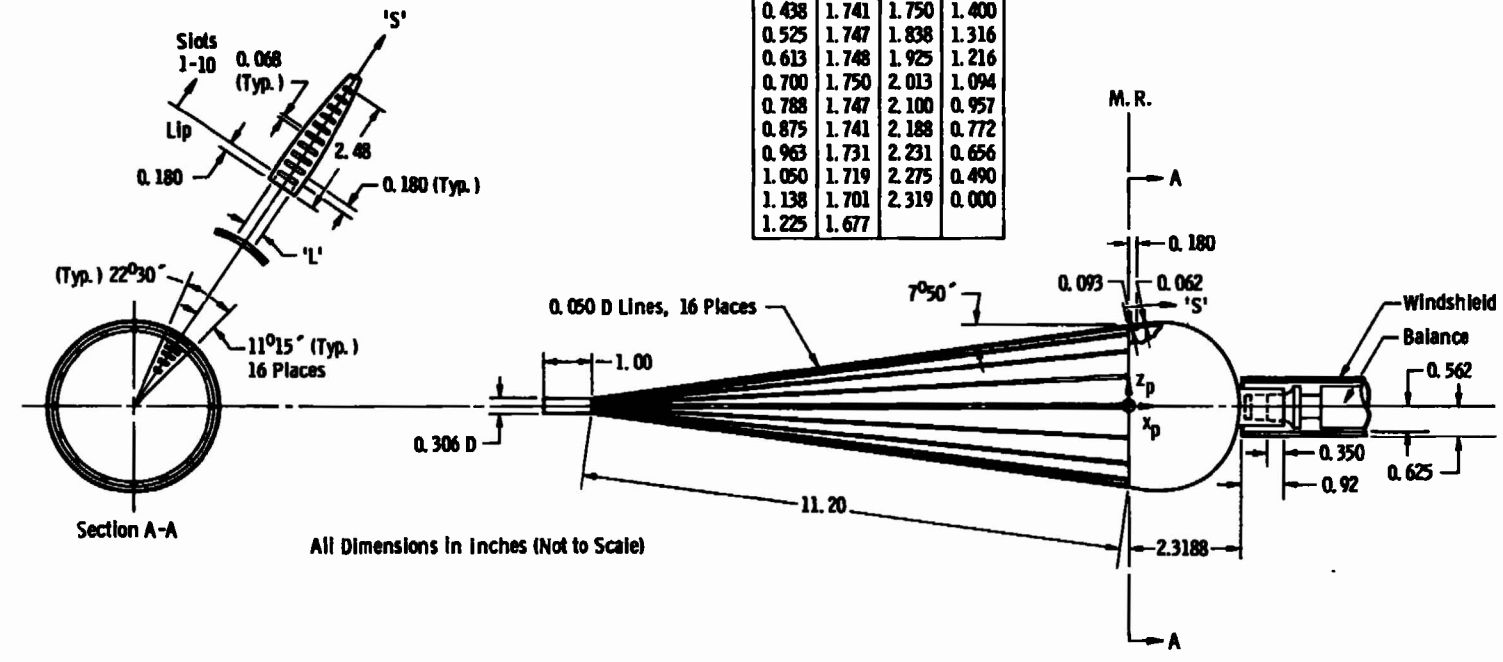

c. Hemisflow Decelerator

Fig. 2 Concluded

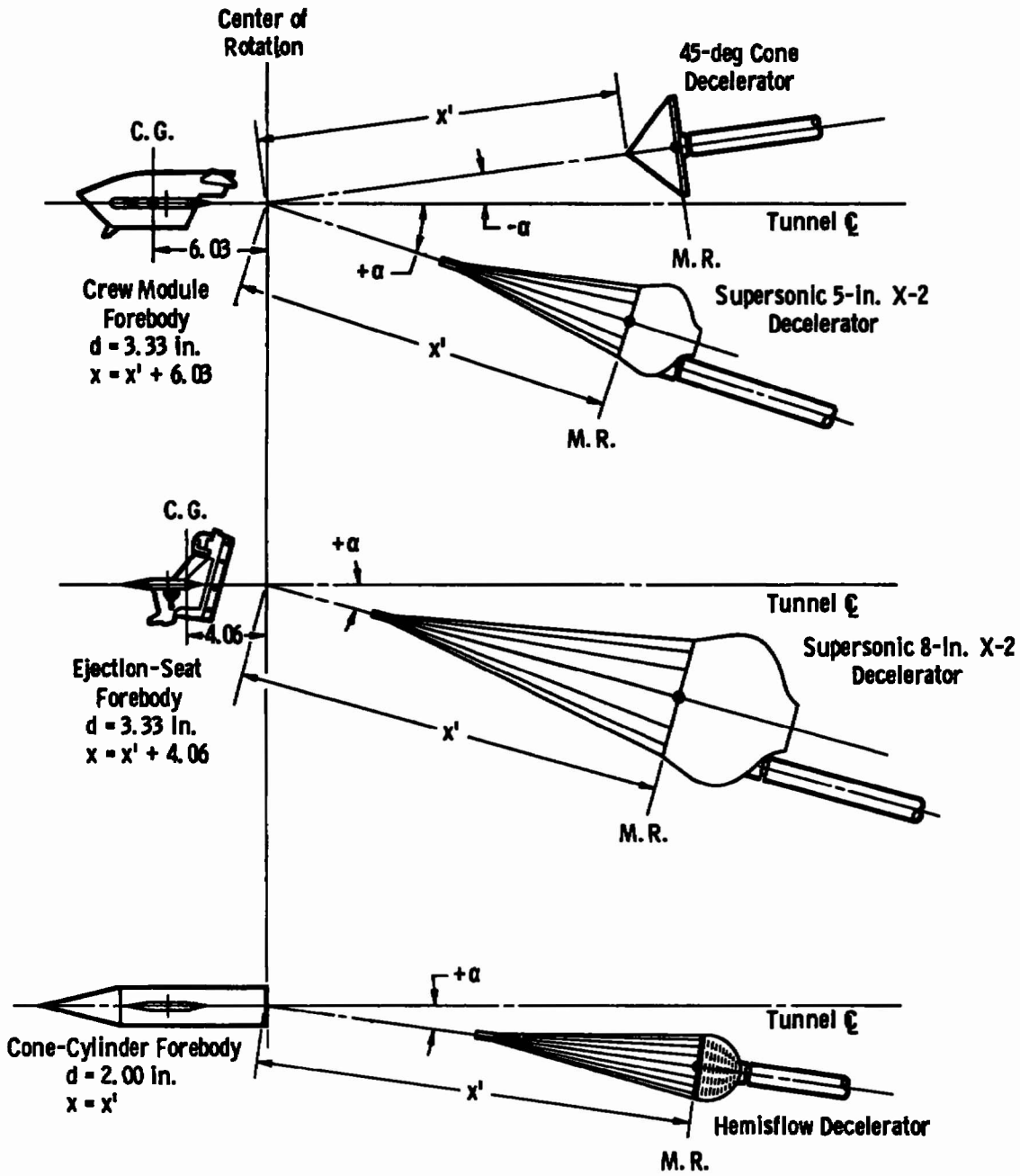

Fig. 3 Schematic of Decelerators Relationship to Forebodies

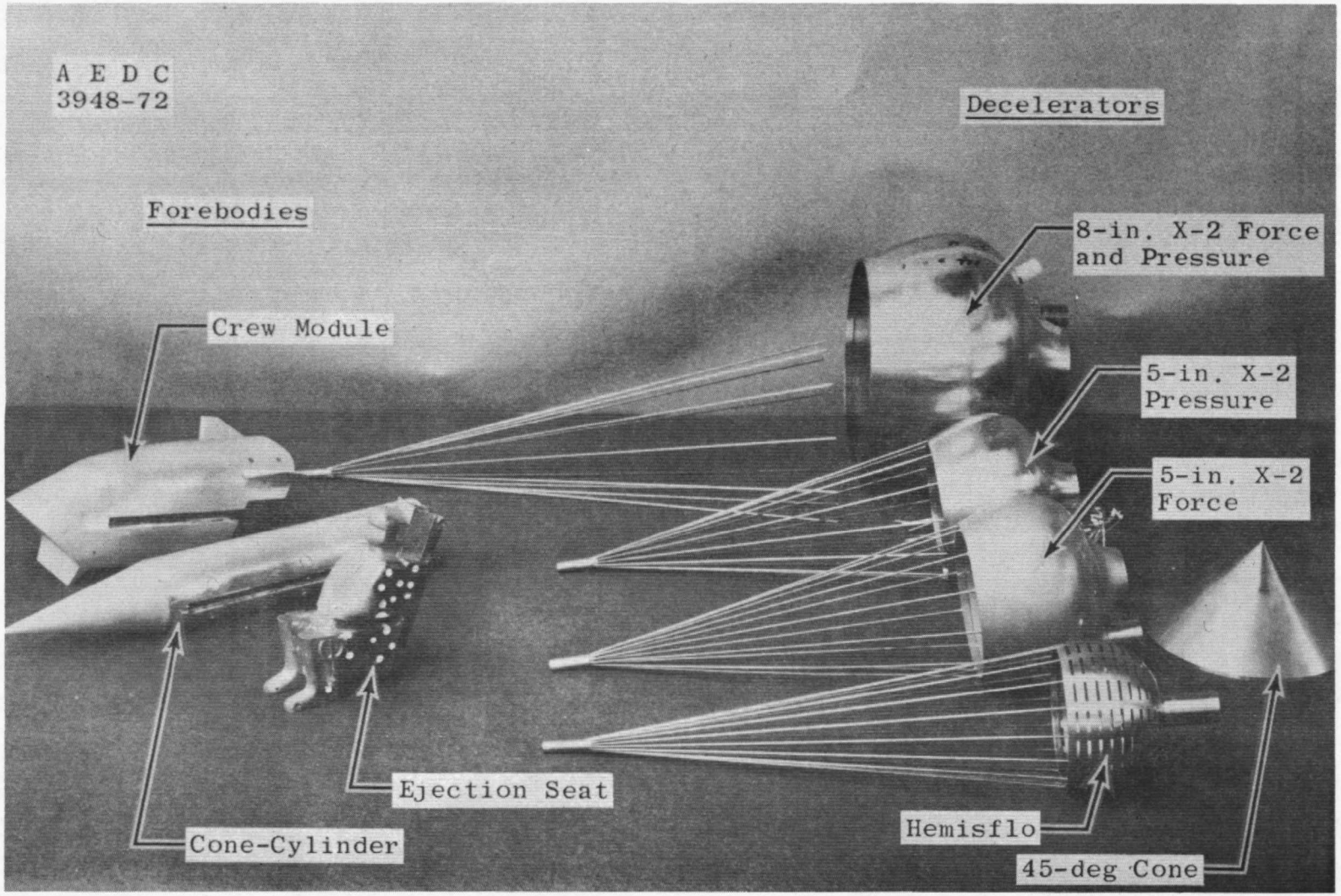

a. Photograph of Forebodies and Decelerators

Fig. 4 Model Photographs

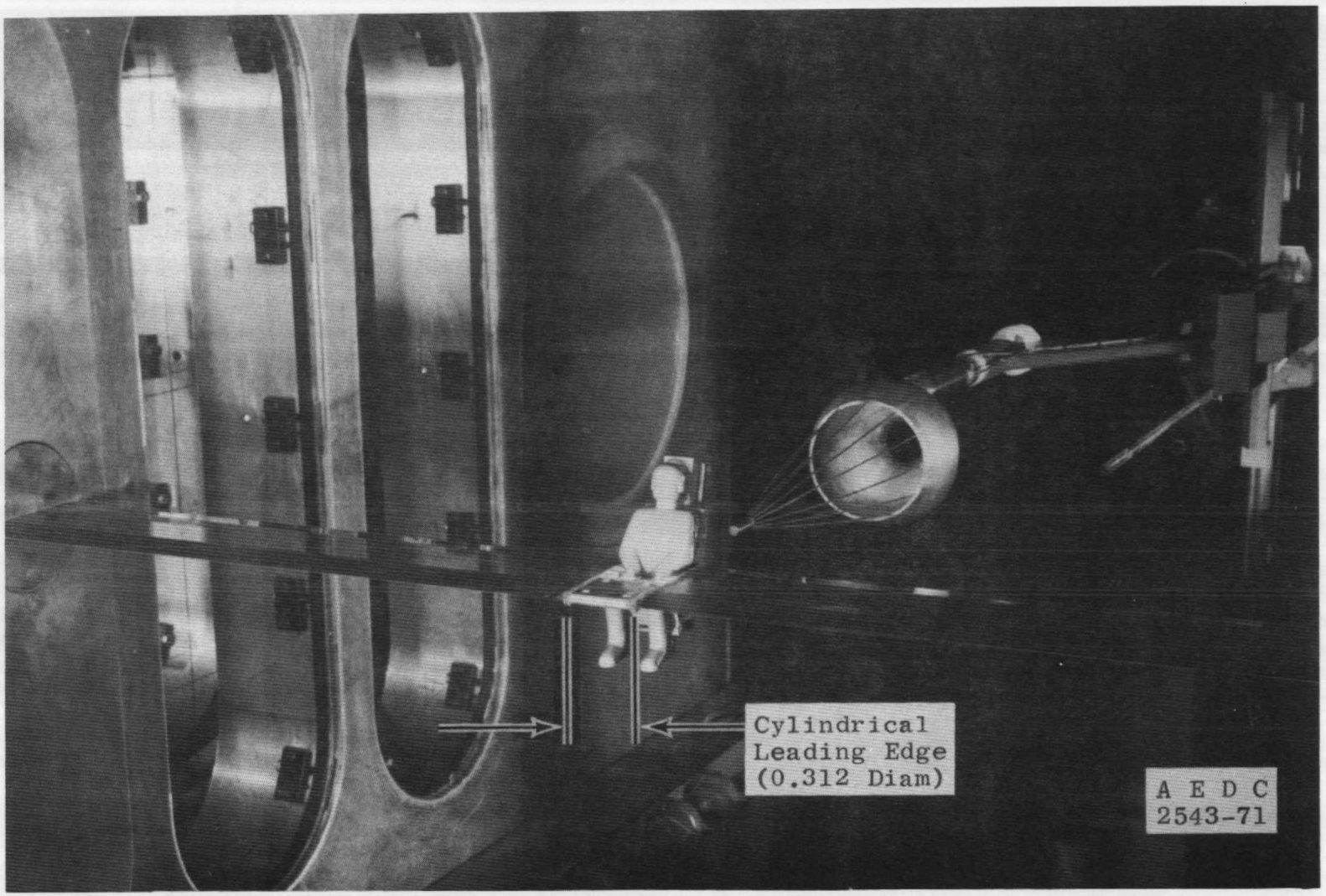

b. Installation of Ejection-Seat Forebody and Supersonic X-2 Decelerator with Lines and without Webs

Fig. 4 Continued

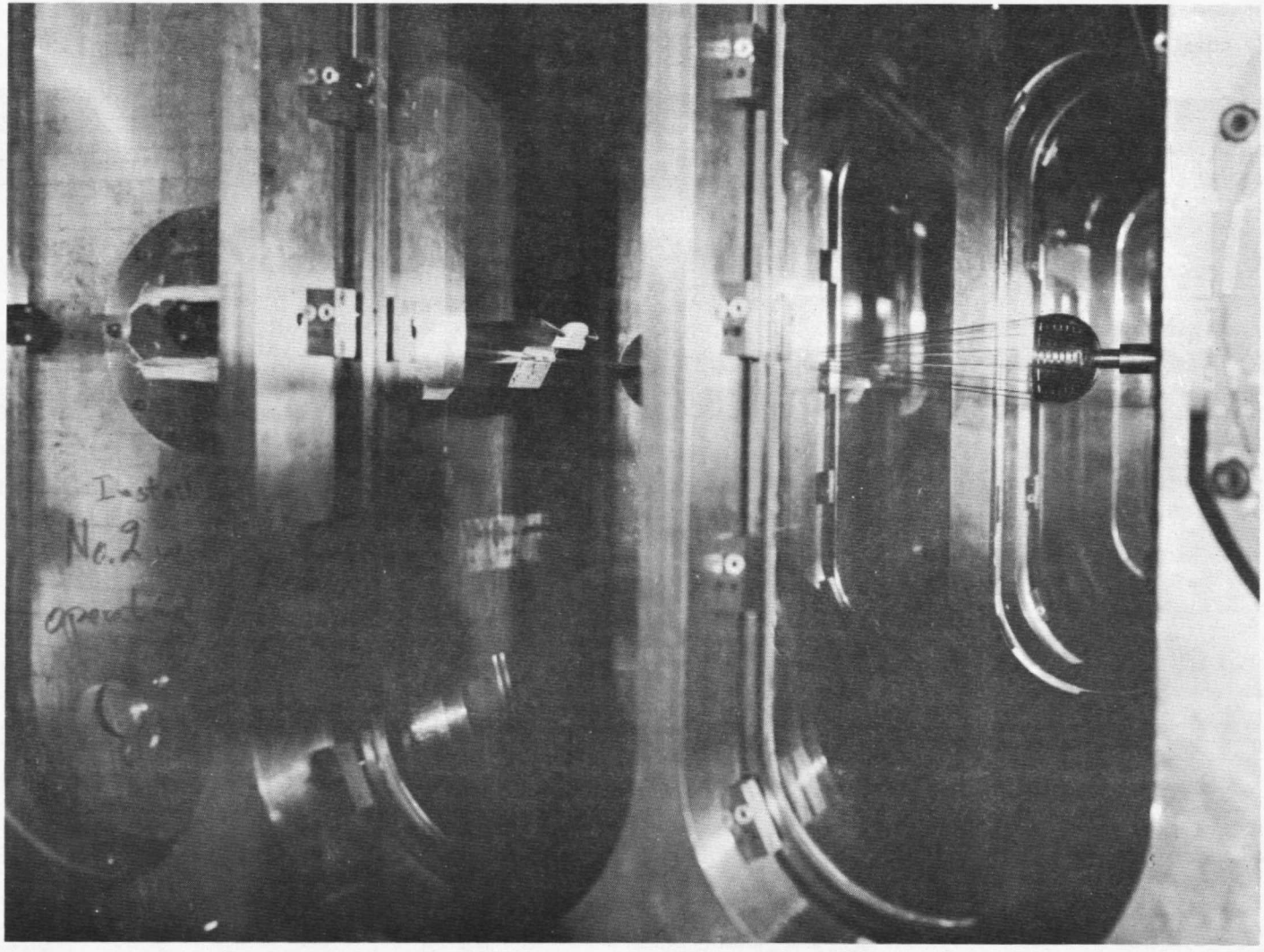

c. Installation of Crew Module Forebody and Hemisflo Decelerator
Fig. 4 Concluded

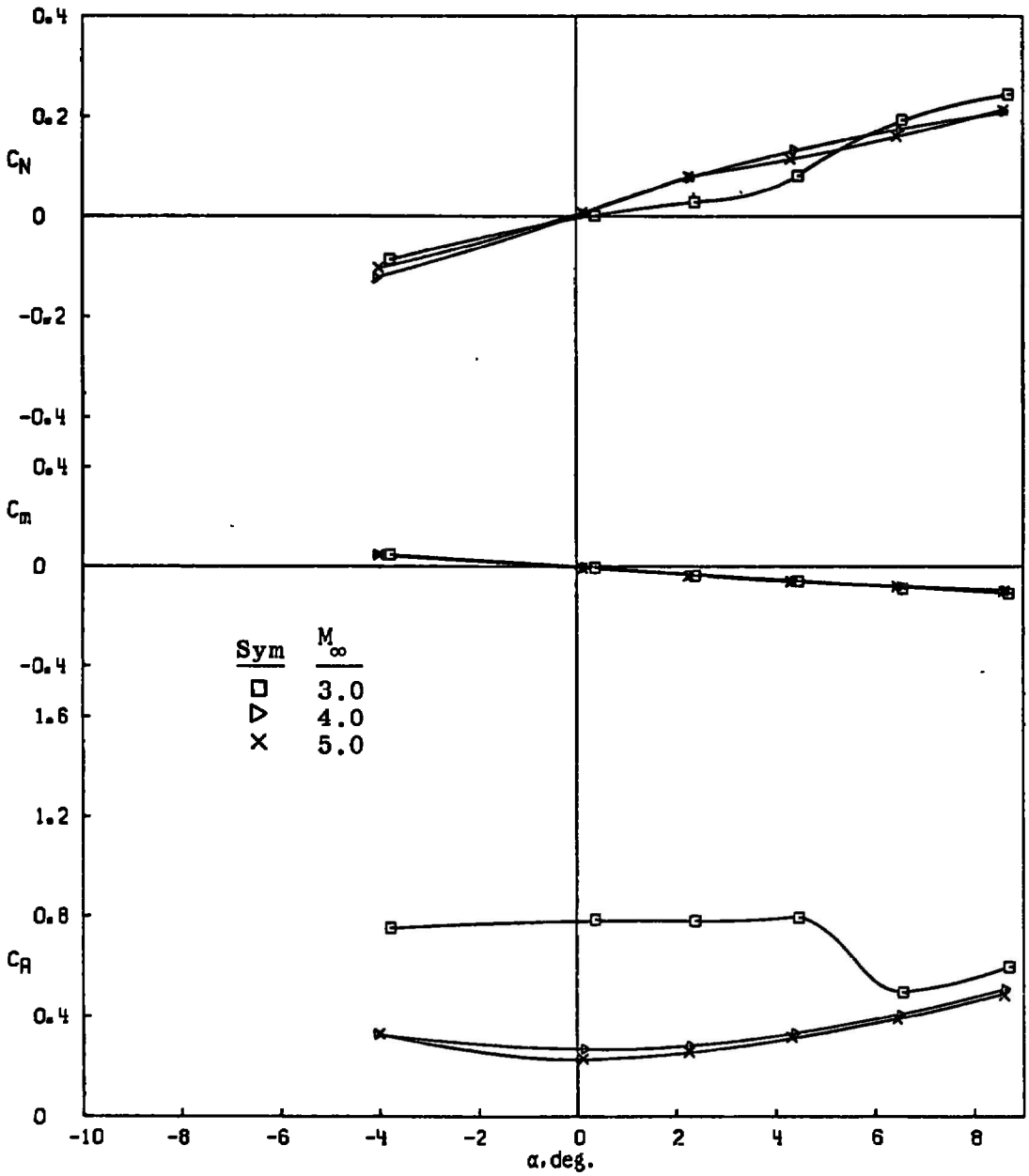

a. In Wake of Cone-Cylinder Forebody, x/d = 9.0

Fig. 5 Static-Stability and Axial-Force Characteristics of 8-in. X-2 with Lines, q_∞ = 1.0

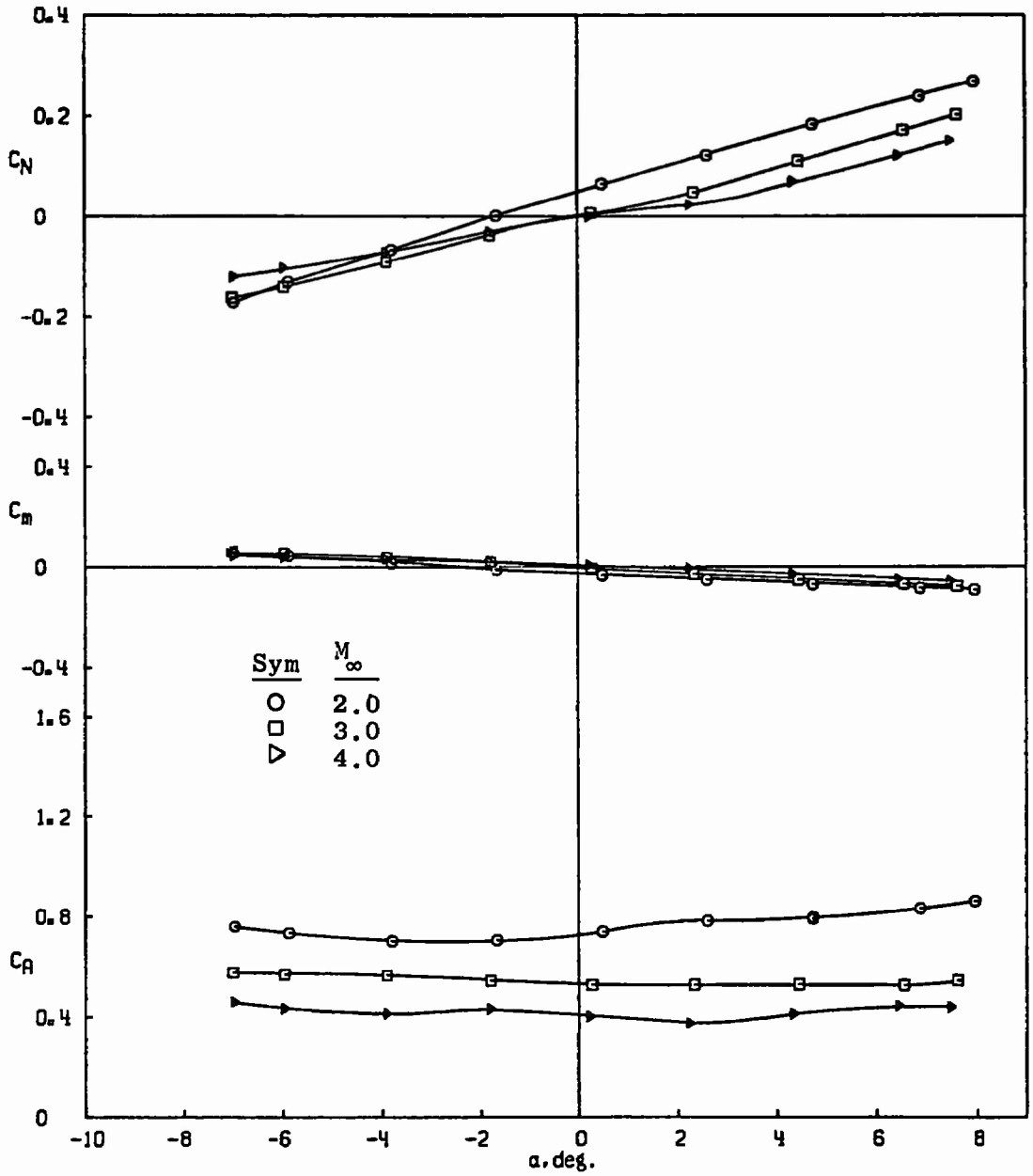

b. In Wake of Ejection Seat Forebody, x/d = 7.0
Fig. 5 Continued

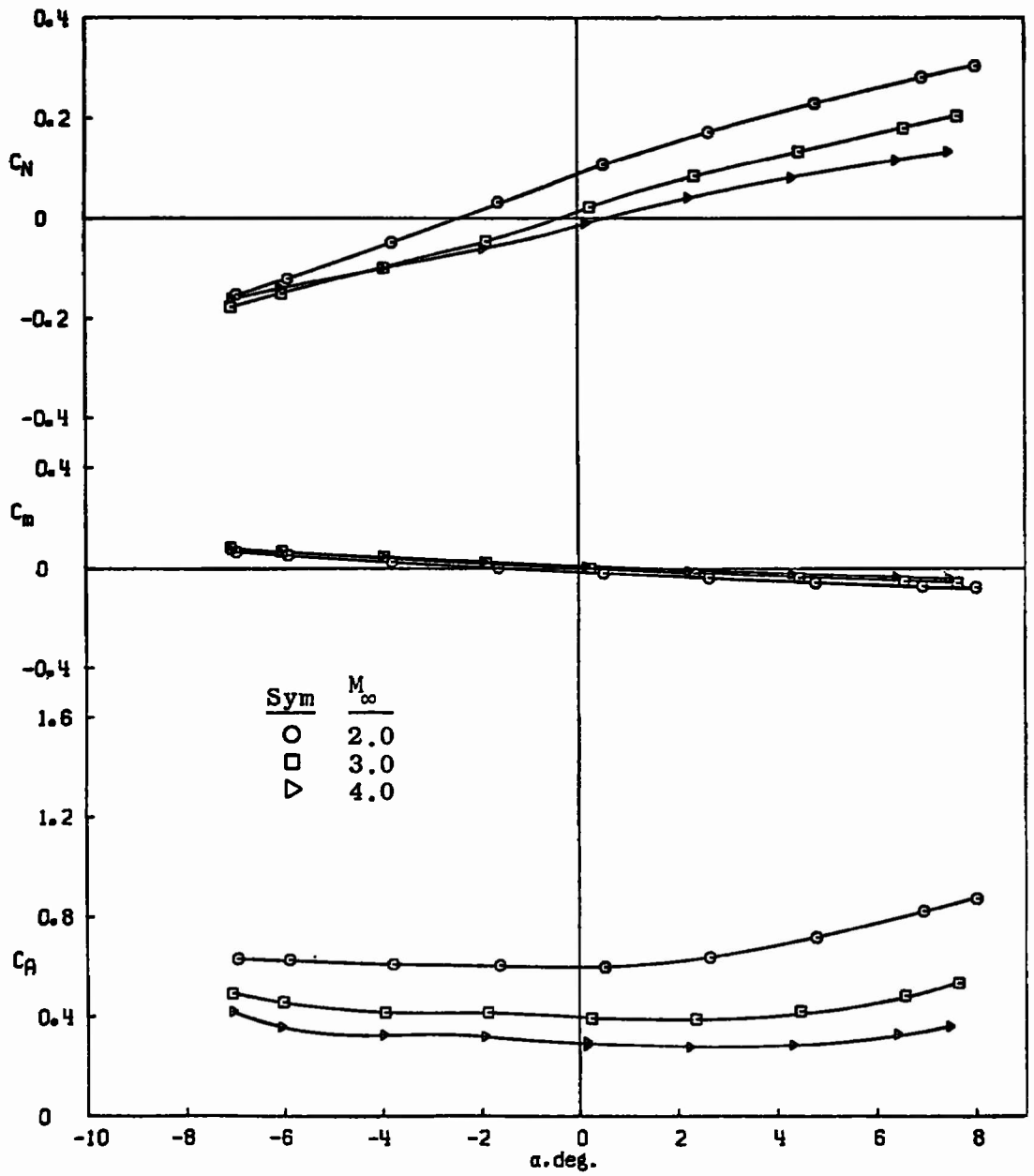

c. In Wake of Crew Module Forebody, x/d = 7.0
Fig. 5 Concluded

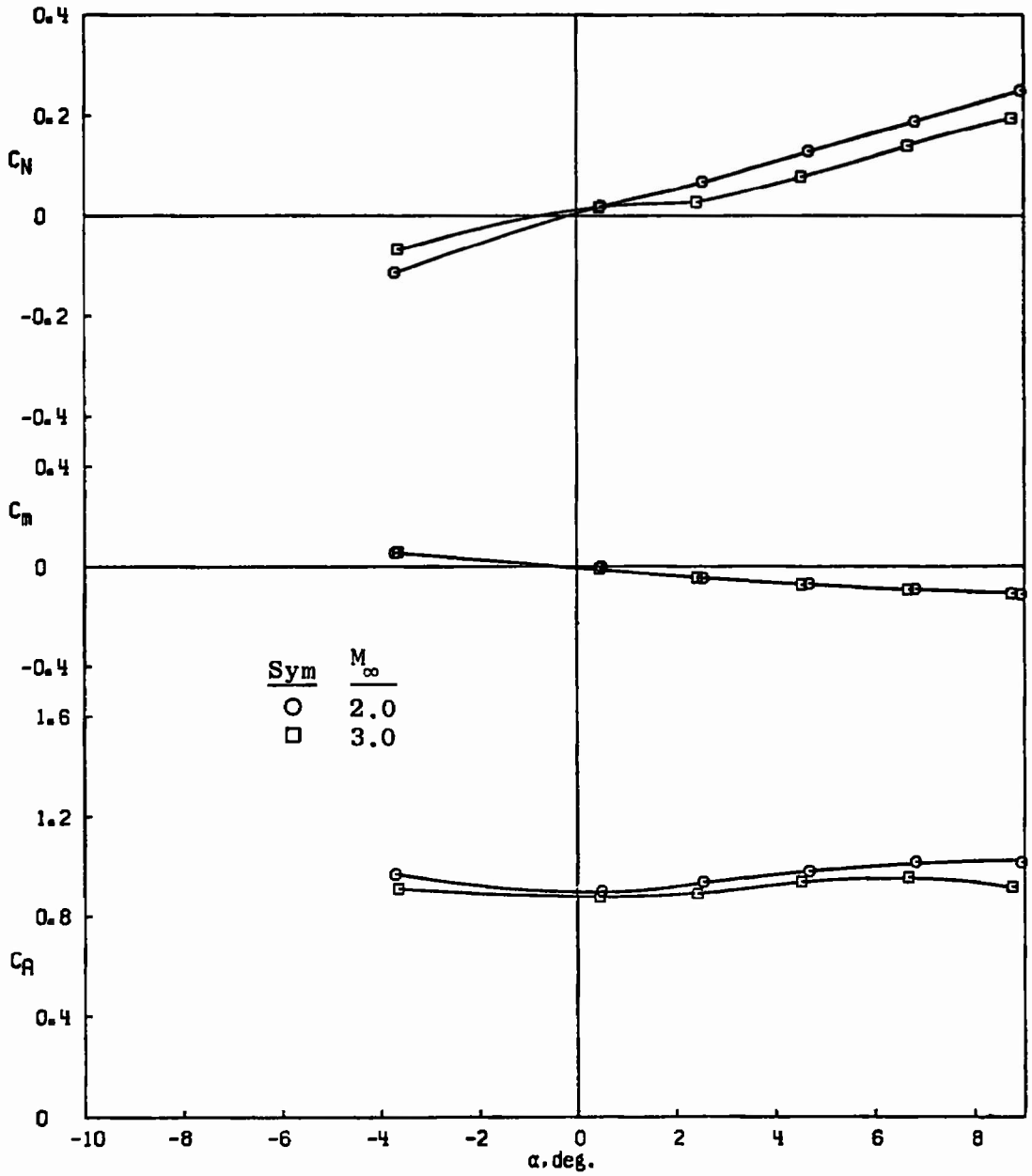

Fig. 6 Static-Stability and Axial-Force Characteristics of 8-in. X-2 without Lines in Wake of Cone-Cylinder Forebody, q_∞ = 1.0, x/d = 9.0

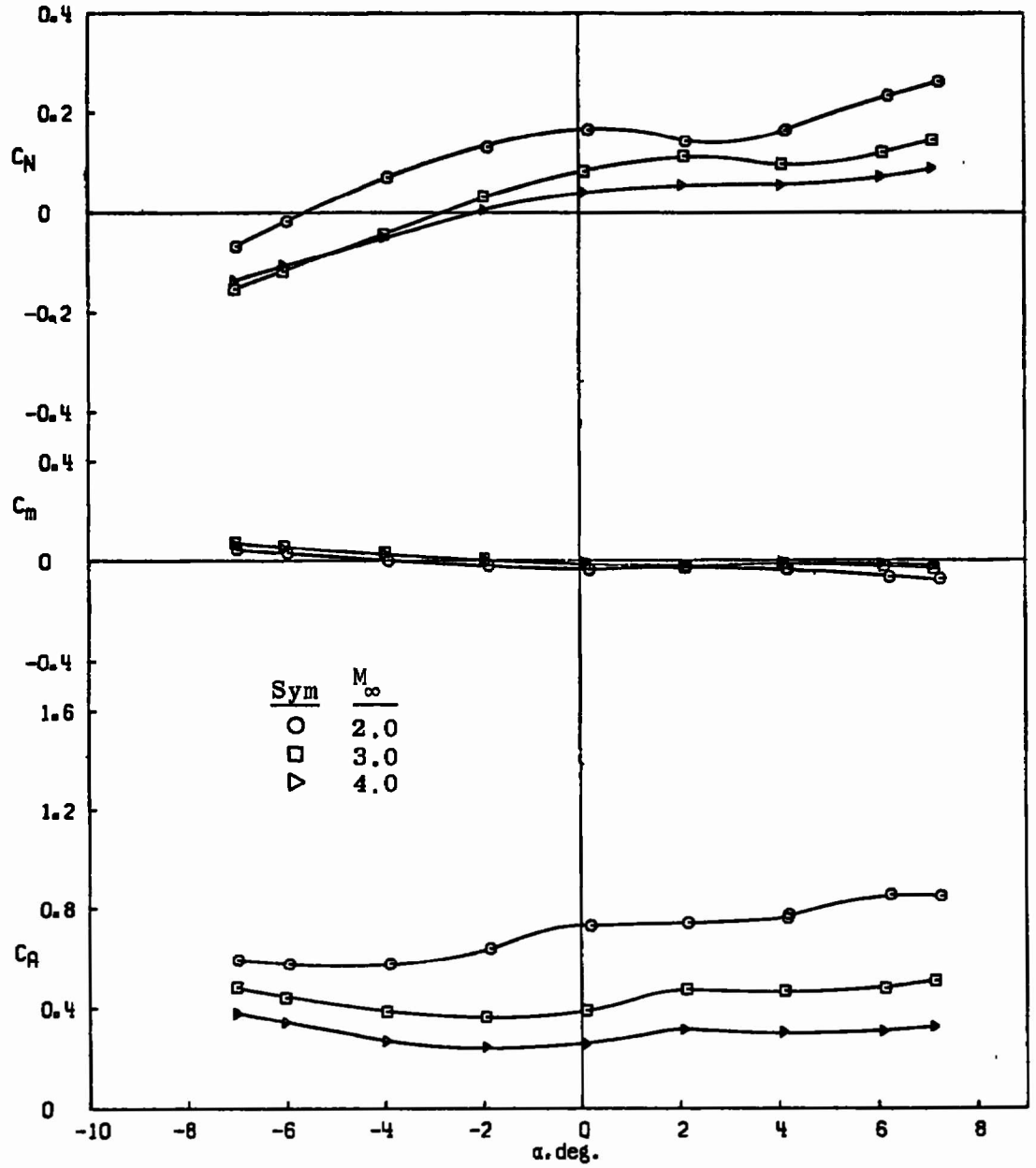

Fig. 7 Static Stability and Axial-Force Characteristics of 5-in. X-2 with Lines in Wake of Crew Module Forebody, q_∞ = 1.0, x/d = 7.0

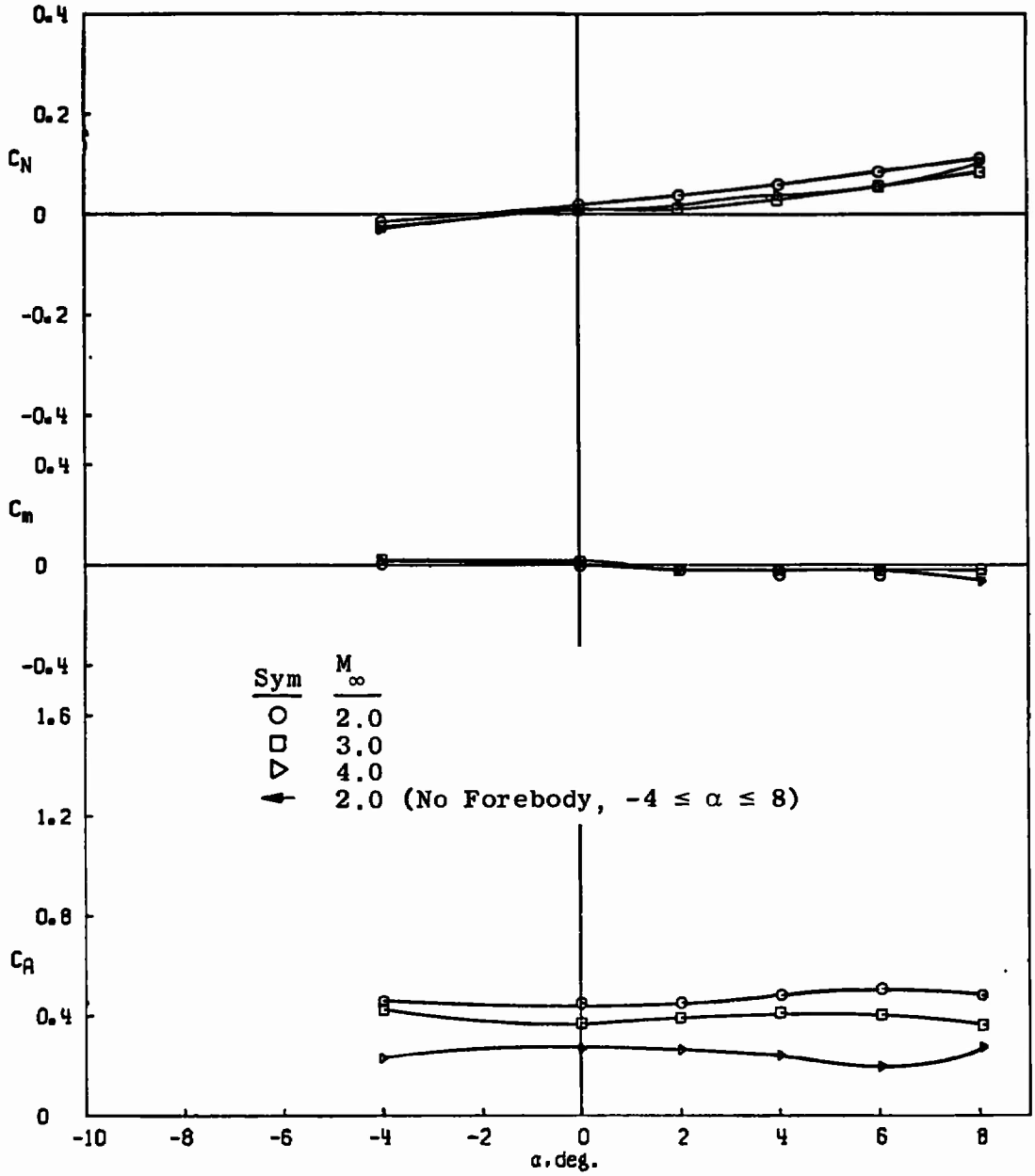

a. In Wake of Cone-Cylinder Forebody, x/d = 7.0

Fig. 8 Static-Stability and Axial-Force Characteristics of Hemisflo Decelerator, q_∞ = 1.0

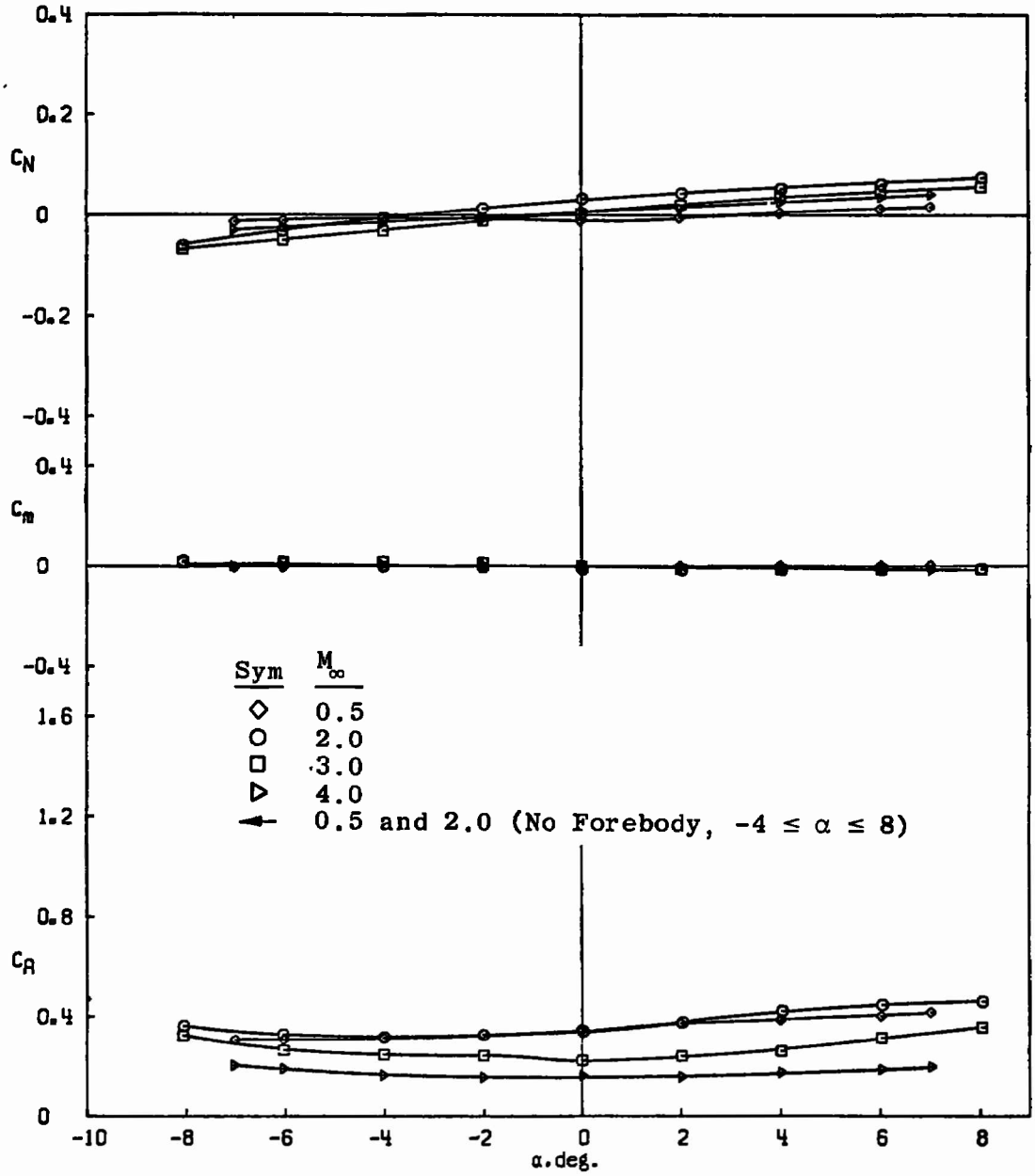

b. In Wake of Ejection Seat Forebody, x/d = 7.0
Fig. 8 Continued

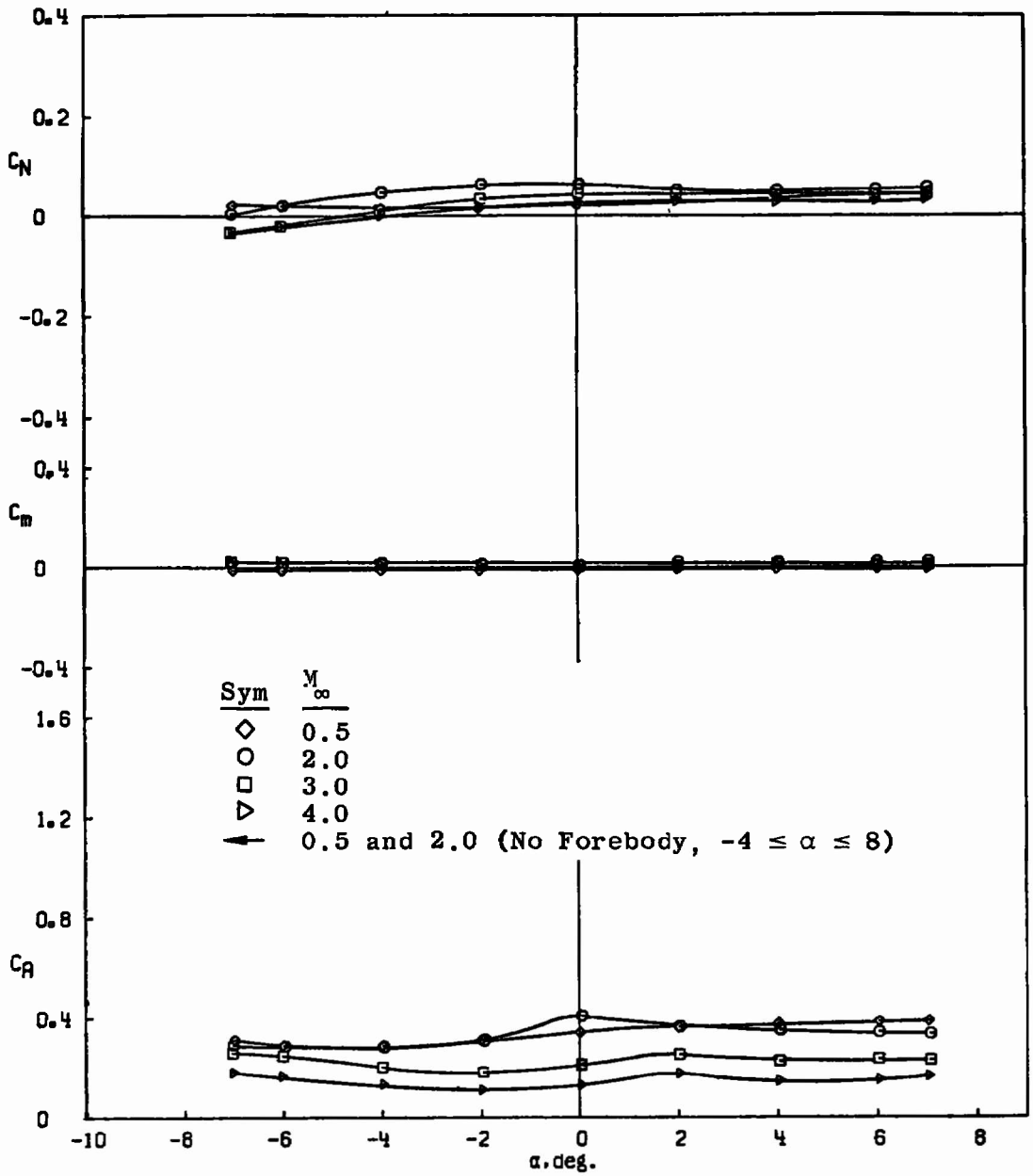

c. In Wake of Crew Module Forebody, x/d = 7.0
Fig. 8 Concluded

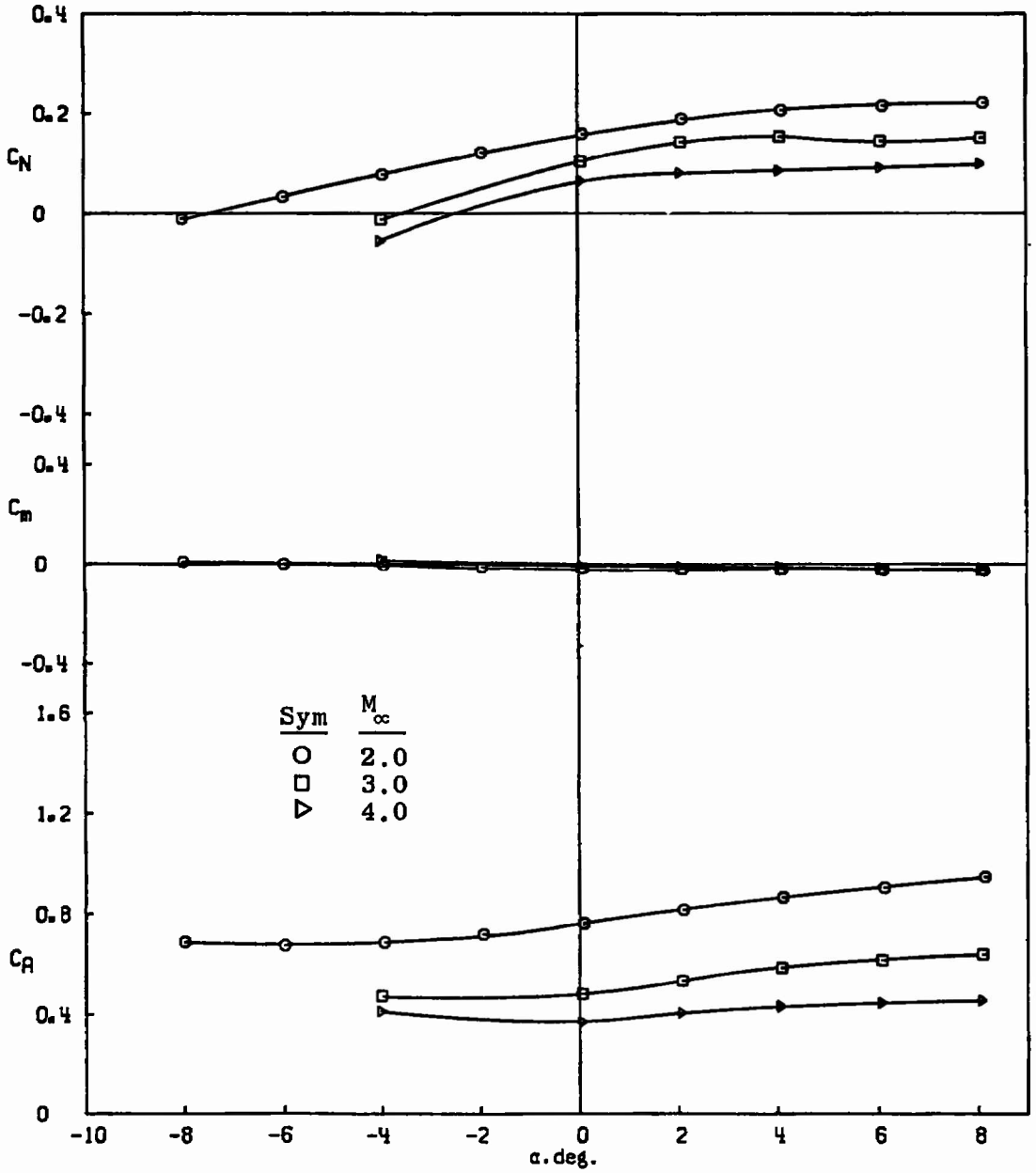

a. x/d = 4.0

Fig. 9 Static-Stability and Axial-Force Characteristics of 45-deg Conical Decelerator in Wake of Crew Module Forebody, q_∞ = 1.0

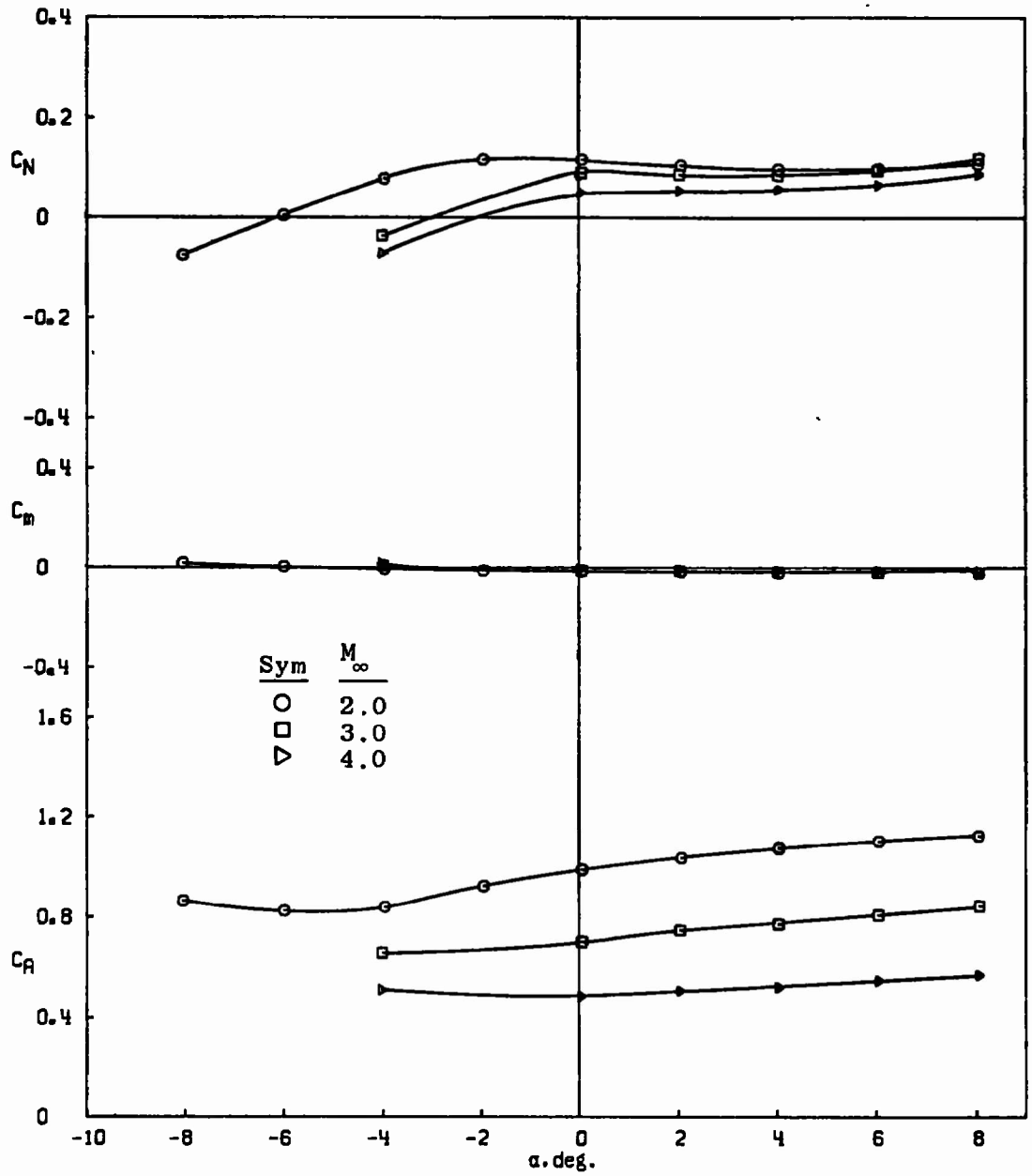

b. x/d = 7.0
Fig. 9 Concluded

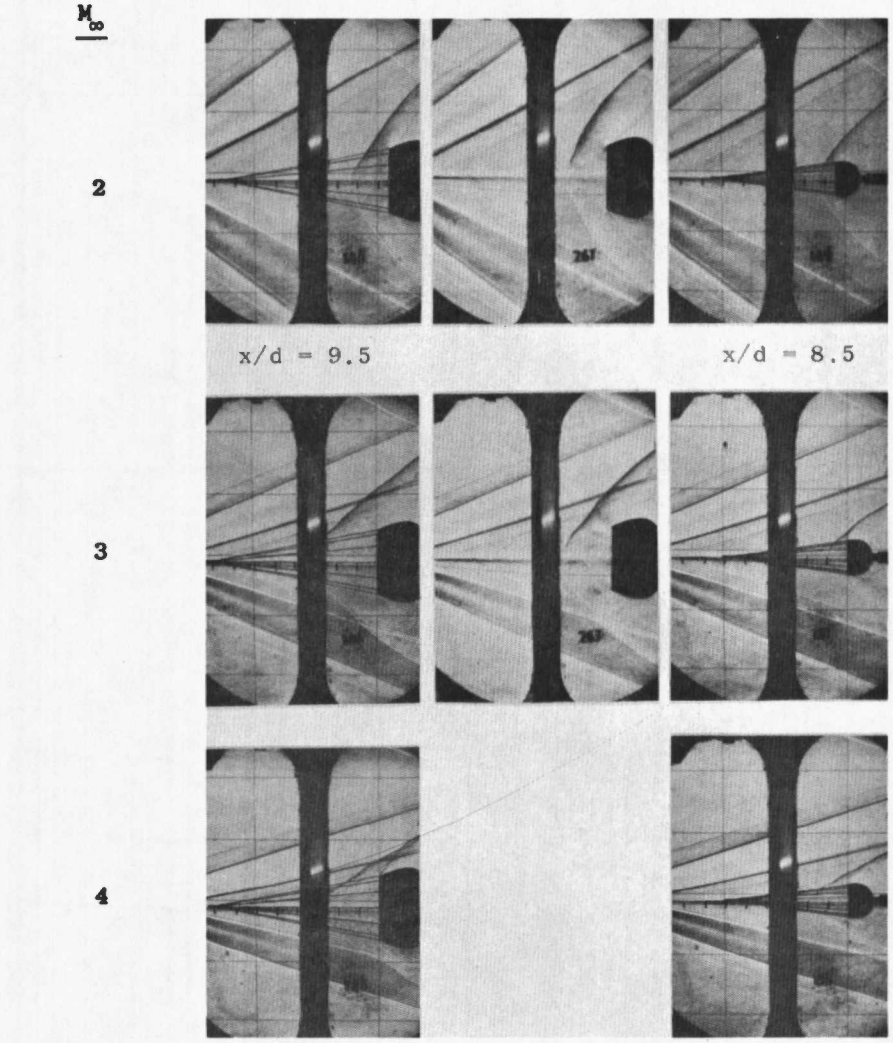

a. Cone-Cylinder, x/d = 9.0

Fig. 10 Schlieren Photographs of Decelerators in Wake of Forebodies, q_∞ = 1.0

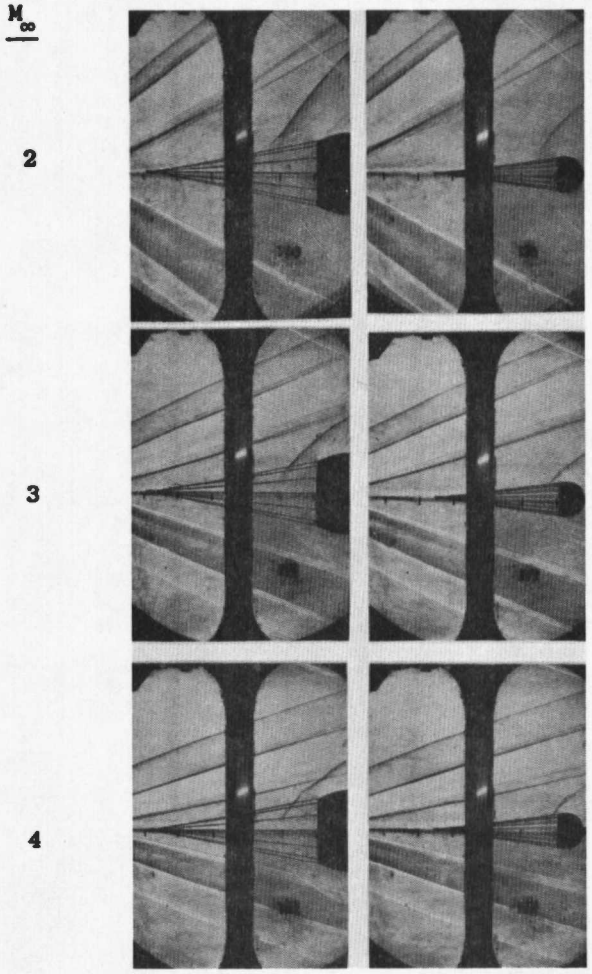

b. Ejection Seat, x/d = 7.0
Fig. 10 Continued

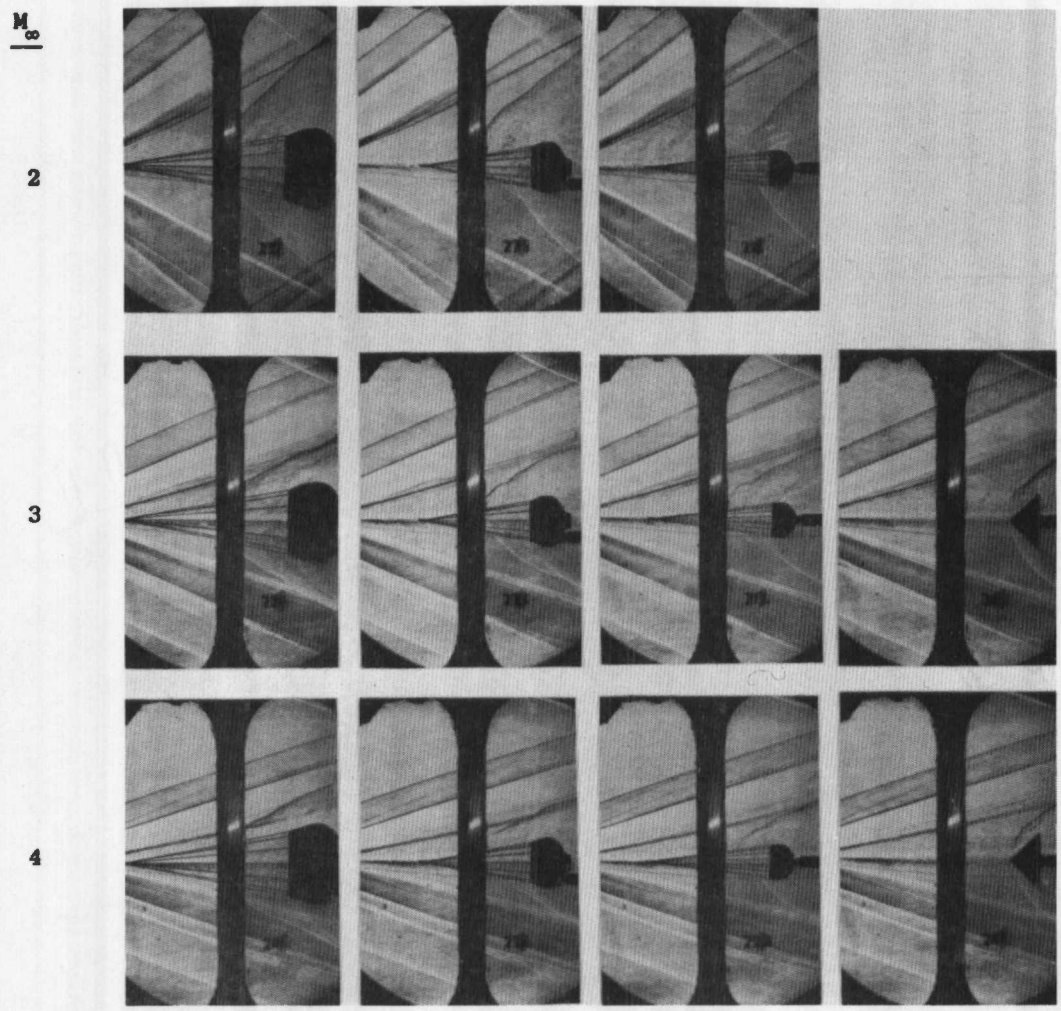

c. Crew Module, x/d = 7.0
Fig. 10 Concluded

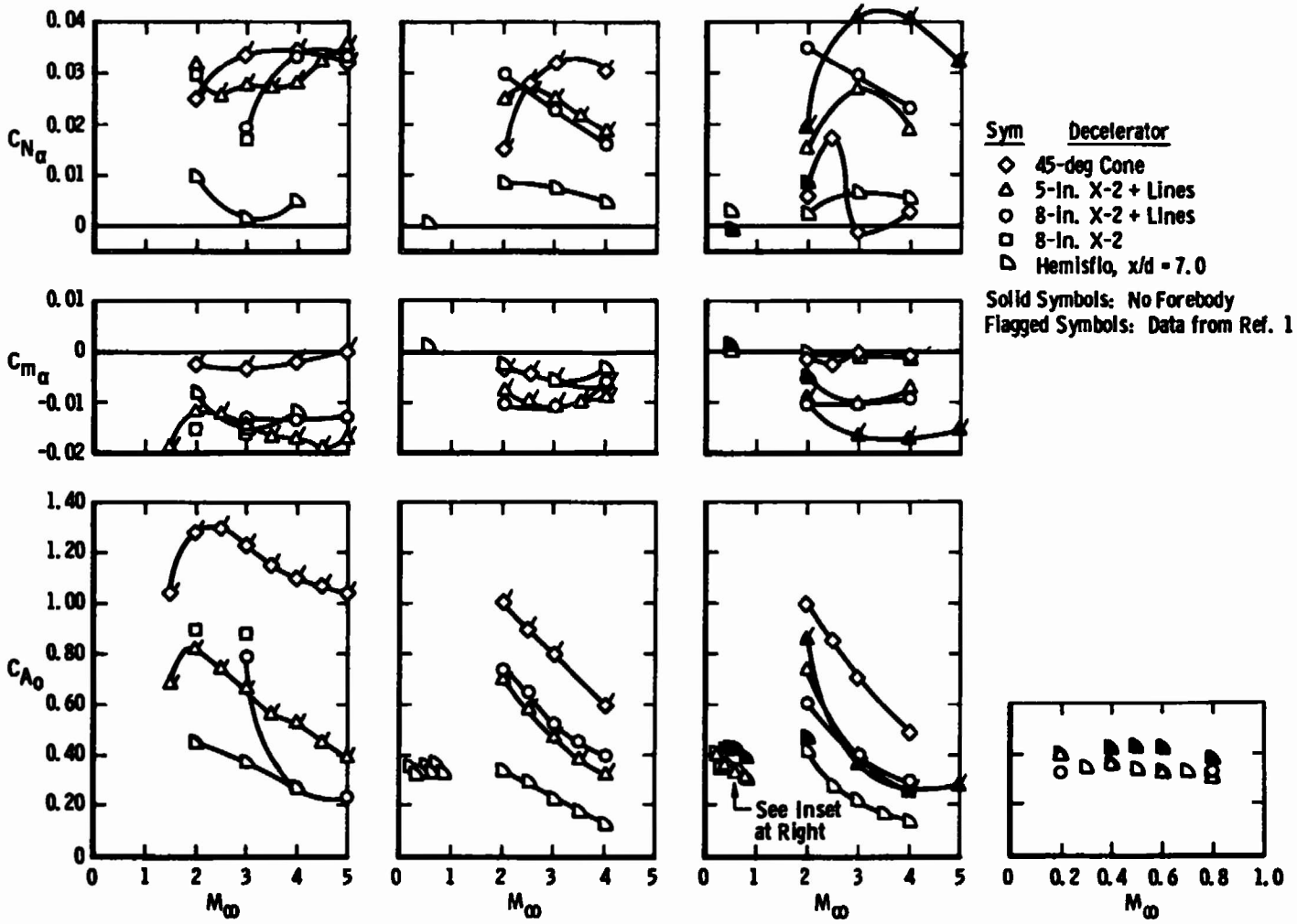

a. In Wake of Cone-Cylinder x/d = 9.0

b. In Wake of Ejector Seat x/d = 7.0

c. In Wake of Crew Module x/d = 7.0

Fig. 11 Effect of Mach Number on Stability Derivatives and Axial Force at Zero Pitch Angle for Several Decelerators, q_∞ = 1.0

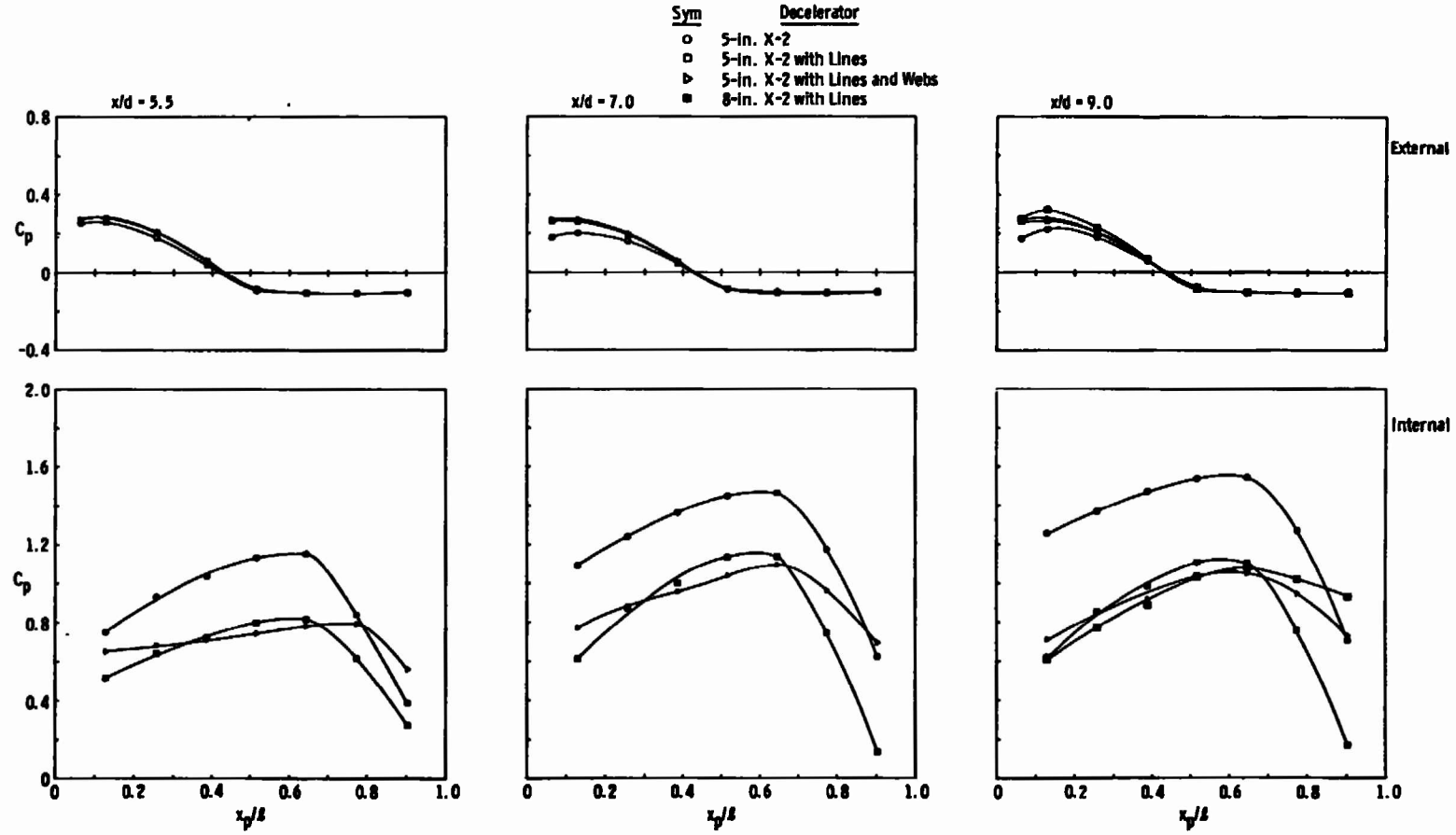

a. $M_\infty = 3.0$

Fig. 12 Zero Pitch Angle Pressure Distributions on Supersonic X-2 Decelerators in Wake of Cone-Cylinder Forebody, $q_\infty = 1.0$

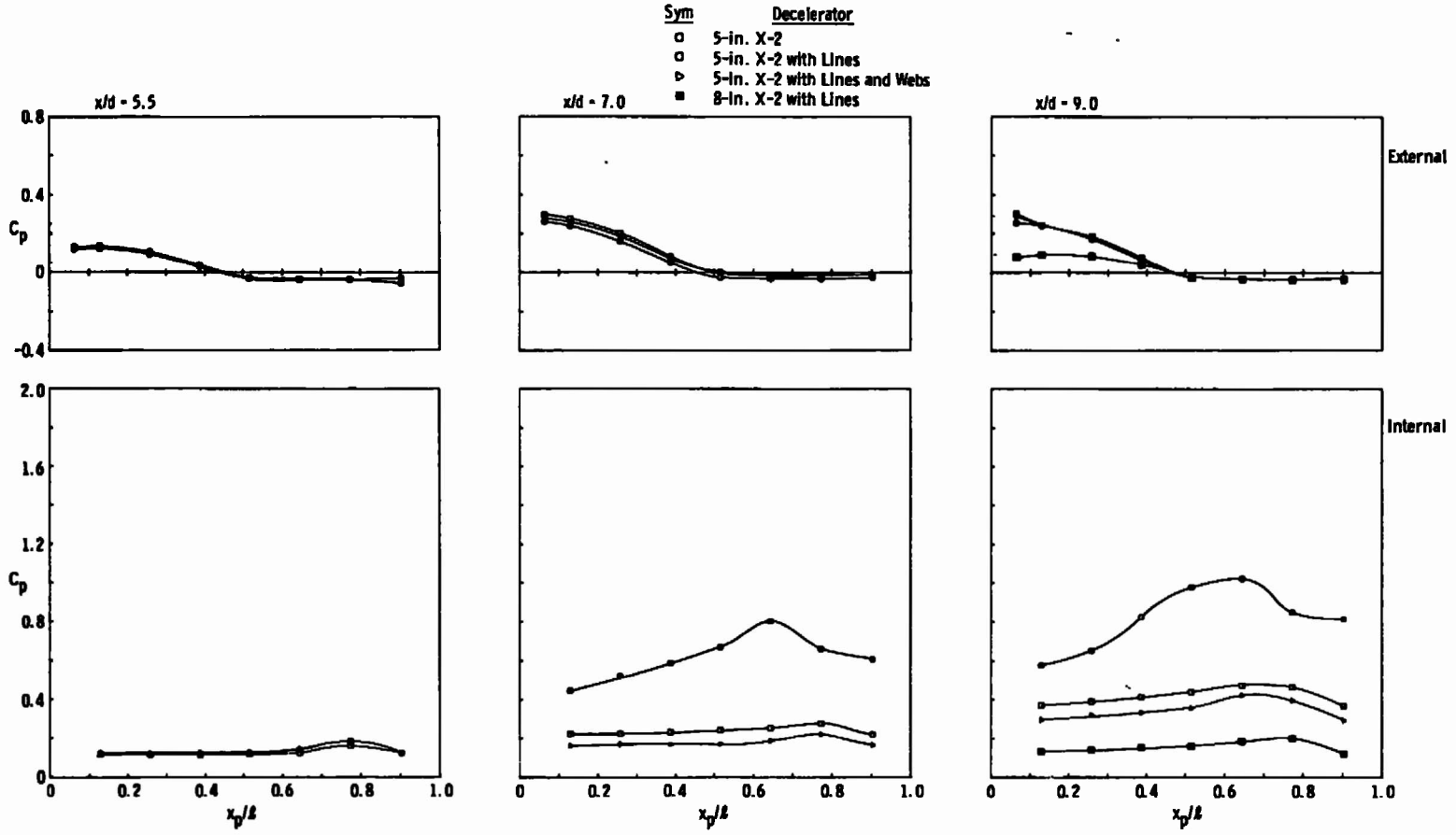

b. $M_\infty = 5.0$

Fig. 12 Concluded

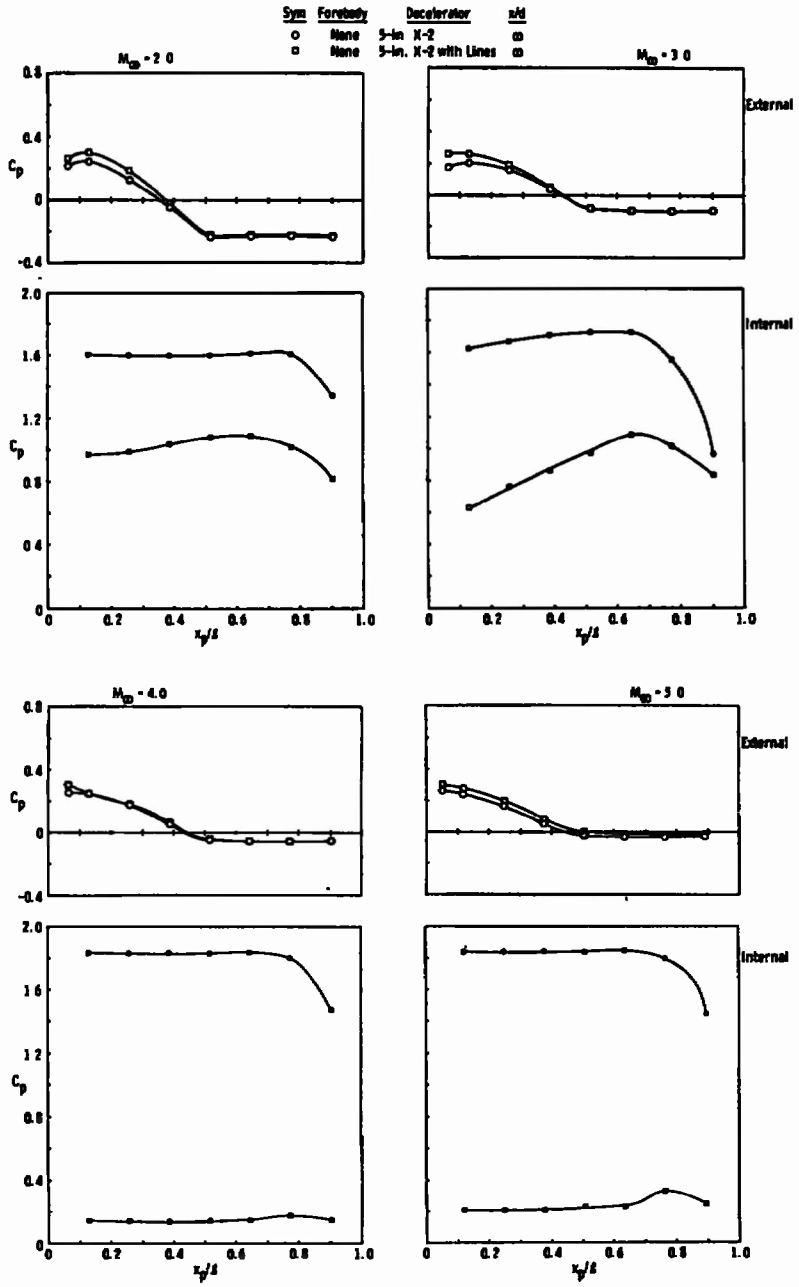

Fig. 13 Zero Pitch Angle Pressure Distributions on 5-in. Supersonic X-2 Decelerator in the Free Stream, q_∞ = 1.0

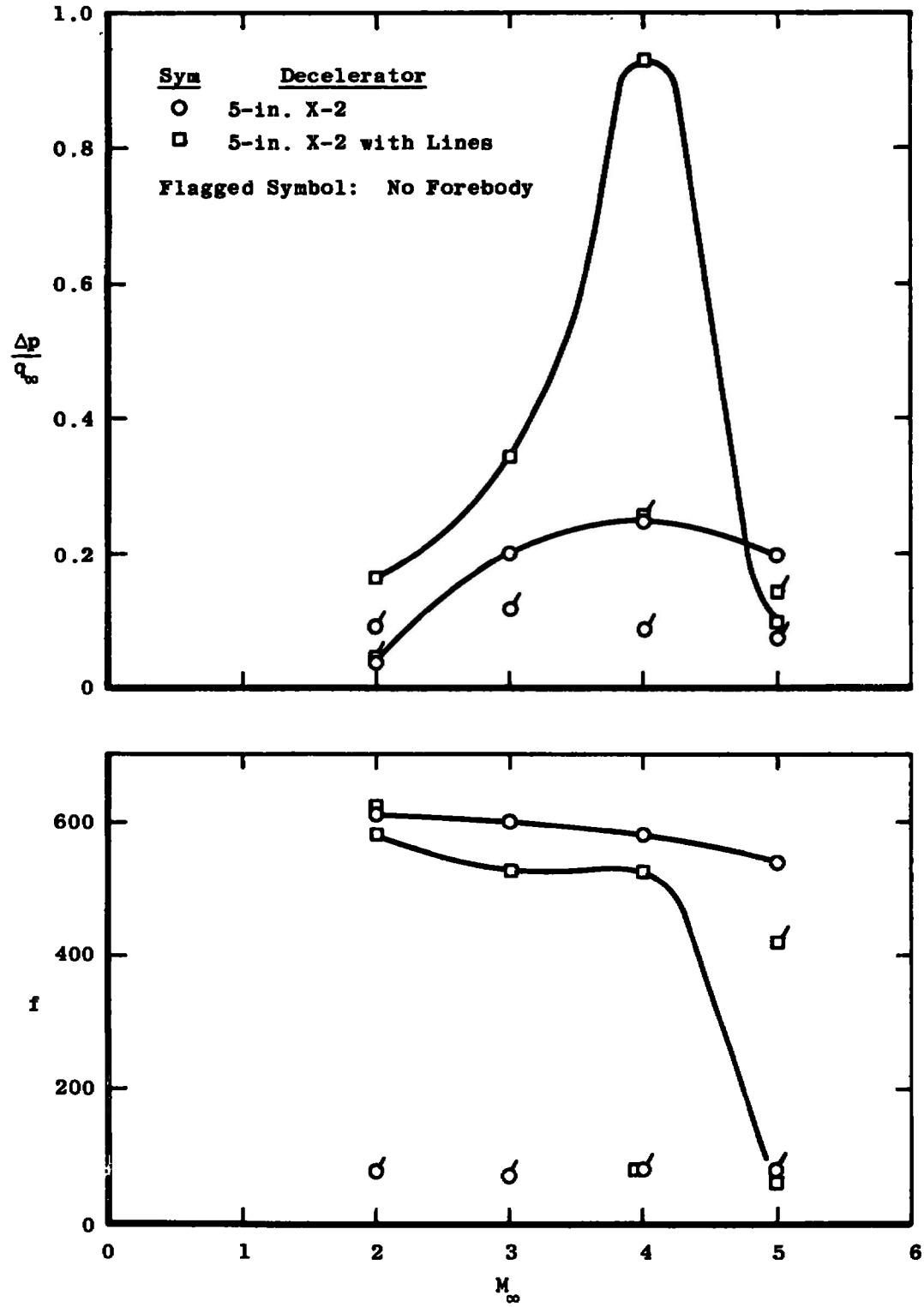

Fig. 14 Internal Pressure Fluctuations at $x_p/\ell = 0.735$ on X-2 Decelerator in Wake of Cone-Cylinder, x/d = 7.0, $\overline{q_\infty = 1.0}$

TABLE I
TEST CONDITIONS

Nominal M_∞	Calibrated M_∞	p_0, psia	p_∞, psia	T_0, °R	q_∞, psia	Re/in. x 10^{-6}
0.2	0.19	18.0	17.55	545	0.4	0.128
0.3	0.31	16.9	15.80	545	1.1	0.191
0.4	0.40	10.0	9.00	545	1.0	0.141
0.5	0.51	6.7	5.65	545	1.0	0.116
0.6	0.61	5.0	3.94	545	1.0	0.100
0.7	0.67	4.0	2.93	540	0.9	0.084
0.8	0.79	3.4	2.25	545	1.0	0.078
1.5	1.49	2.3	0.636	560	1.0	0.055
2.0	1.99	2.8	0.363	560	1.0	0.058
2.5	2.49	3.9	0.232	570	1.0	0.063
3.0	3.00	5.8	0.158	580	1.0	0.066
3.5	3.49	8.8	0.117	590	1.0	0.079
4.0	4.00	6.8	0.045	610	0.5	0.045
4.0	4.00	13.6	0.090	610	1.0	0.086
4.0	4.01	20.5	0.133	610	1.5	0.131
4.0	4.02	27.4	0.176	610	2.0	0.173
5.0	5.02	30.2	0.056	640	1.0	0.114

TABLE II
TEST SUMMARY

1. MODEL CONFIGURATION CODE

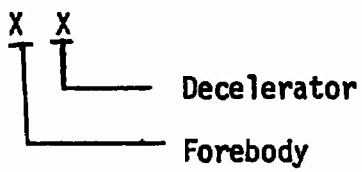

FOREBODY CODE	DECELERATOR CODE
0 - Cone-Cylinder	1 - 45 deg cone
1 - Ejection seat	2 - 5 in. X-2
2 - None	3 - 5 in. X-2 with lines
3 - Crew module	4 - 5 in. X-2 with lines and webs
	5 - 8 in. X-2 with lines
	6 - 8 in. X-2
	7 - Hemisflo

2. ANGLE-OF-ATTACK CODE, deg

0
+ → 0,2,4,6,8
± → 0,±2,±4,±6,±8

3. X/D TRAVERSE CODE

A - 9.0, 9.5, 10.0, 10.5, 11.0
B - 2.5, 3.0, 4.0, 5.0, 6.0, 7.0, 8.0, 9.0, 10.0, 11.0
C - 6.5, 7.0, 7.5, 8.0, 8.5, 9.0
D - 4.5, 5.0, 6.0, 7.0
E - 5.6, 6.0, 7.0
F - 5.0, 6.0, 7.0
G - 6.5, 7.0
H - 4.0, 5.0, 7.0
I - 4.0, 5.0, 6.0, 7.0, 8.0, 8.4
J - 5.5, 7.0, 9.0
K - 4.0, 5.5, 7.0, 9.0
L - 3.0, 5.5, 7.0, 9.0
M - 4.0, 4.5, 5.0, 5.5, 6.0, 6.5, 7.0, 9.0
N - 9.0, 10.0

TABLE II (Continued)

4. TEST MATRIX

a. Force Data (All data at q_∞ = 1.0 psia except as noted)

Config.	Nominal Mach Numbers	x/d	α
7	2.0,3.0,4.0*,5.0	A	0
	3.0,4.0,5.0	9.0	+
8	2.0,3.0	B	0
	2.0,3.0	9.0	+
9	2.0,3.0,4.0	C	0
	2.0,3.0,4.0	7.0	+
17	2.0,2.5,3.0,3.5,4.0	E	0
	2.0,3.0,4.0	7.0	±
19	All Except 5.0	D	0
	0.5,2.0,3.0,4.0	7.0	±
29	0.4,0.6,0.8	No Forebody	0
	0.5,2.0	No Forebody	+
32	2.0,2.5,3.0,4.0	I	0
	2.0	I	±
	2.5,3.0,4.0	H	+
35	0.2**,0.4,0.6,0.8,2.0,4.0	D	0
	2.0,3.0,4.0	7.0	±
37	0.2**,0.4,0.6***,0.8,2.0,3.0,4.0	G	0
	2.0,3.0,4.0	7.0	±
39	All Except 1.5 and 5.0	F	0
	0.5,2.0,3.0,4.0	7.0	±

*Tested also at q_∞ = 0.5, 1.5, and 2.0 psia

**q_∞ = 0.4 psia at M_∞ = 0.2

***x/d = 8.0 and 8.4

TABLE II (Concluded)

4. TEST MATRIX (concluded)

b. Pressure Data (All data at $\alpha = 0°$ and $q_\infty = 1.0$ psia except as noted)

Config.	Nominal Mach Numbers	x/d
3	2.0,4.0[z],5.0	K
	3.0	L
	4.0	M
5	2.0,3.0,4.0[zz],5.0	J
6	2.0,3.0,4.0,5.0	J
7	2.0	10.0
	3.0,4.0,5.0	N
23	2.0,3.0,4.0,5.0	No Forebody
25	2.0,3.0,4.0,5.0	No Forebody

z Tested only at $q_\infty = 0.5$ and 1.5
zz Tested also at $q_\infty = 0.5$ and 1.5

UNCLASSIFIED

Security Classification

DOCUMENT CONTROL DATA - R & D

(Security classification of title, body of abstract and indexing annotation must be entered when the overall report is classified)

1 ORIGINATING ACTIVITY *(Corporate author)*
Arnold Enginnering Development Center
Arnold Air Force Station, Tennessee 37389

2a. REPORT SECURITY CLASSIFICATION
UNCLASSIFIED

2b. GROUP
N/A

3 REPORT TITLE
DRAG, PERFORMANCE, CHARACTERISTICS, AND PRESSURE DISTRIBUTIONS OF SEVERAL RIGID AERODYNAMIC DECELERATORS AT MACH NUMBERS FROM 0.2 TO 5

4 DESCRIPTIVE NOTES *(Type of report and inclusive dates)*
April 25 to May 5, 1972--Final Report

5 AUTHOR(S) *(First name, middle initial, last name)*
R. W. Rhudy and S. S. Baker, ARO, Inc.

6 REPORT DATE	7a. TOTAL NO. OF PAGES	7b. NO. OF REFS
December 1972	50	2

8a. CONTRACT OR GRANT NO	9a. ORIGINATOR'S REPORT NUMBER(S)
b. PROJECT NO	AEDC-TR-72-171
c. Program Element 62201F	9b. OTHER REPORT NO(S) *(Any other numbers that may be assigned this report)*
d.	ARO-VKF-TR-72-119

10 DISTRIBUTION STATEMENT Distribution limited to U. S. Government agencies only; this report contains information on test and evaluation of military hardware; December 1972; other requests for this document must be referred to AFFDL(FER), Wright-Patterson Air Force Base, Ohio 45433.

11 SUPPLEMENTARY NOTES	12 SPONSORING MILITARY ACTIVITY
Available in DDC	AFFDL(FER) Wright-Patterson Air Force Base Ohio 45433

13 ABSTRACT

Static force and pressure distribution tests were conducted at Mach numbers from 0.2 to 5.0 on rigid models of several aerodynamic decelerators in the wake of three types of forebodies. The tests were conducted at decelerator pitch angles from -8 to 8 deg at nominal free-stream dynamic pressures of 0.5, 1.0, 1.5, and 2.0 psia. The decelerators were positioned at avrious axial stations in the wake of the forebodies, and selected configurations were tested in the free stream (no forebodies). Data are presented showing the effects of Mach numbers, decelerator pitch angle, and location in the wake on the drag and stability of various decelerator configurations. The pressure data support the measured force data and show large fluctuations in the canopy internal pressure on the supersonic X-2 parachute design.

Distribution limited to U. S. Government agencies only; this report contains information on test and evaluation of military hardware; December 1972; other requests for this document must be referred to AFFDL(FER), Wright-Patterson Air Force Base, Ohio 45433.

DD FORM 1 NOV 65 1473

UNCLASSIFIED

Security Classification

14. KEY WORDS	LINK A		LINK B		LINK C	
	ROLE	WT	ROLE	WT	ROLE	WT
decelerators						
parachutes						
conical bodies						
drag						
stability						
performance characteristics						
supersonic wind tunnels						